Leptonic τ decays: How to determine the Lorentz structure of the charged leptonic weak interaction by experiment

Wulf Fetscher
Institut für Mittelenergiephysik, Eidgenössische Technische Hochschule Zürich, CH-5232 Villigen PSI, Switzerland
(Received 15 May 1990)

The purely leptonic decays $\tau^+ \to \mu^+ \nu_\mu \bar{\nu}_\tau$ and $\tau^+ \to e^+ \nu_e \bar{\nu}_\tau$ are both described by the most general (local, derivative-free, lepton-number-conserving) four-fermion interaction Hamiltonian characterized by ten complex coupling constants. The $V-A$ hypothesis of the standard model can be proven experimentally, as has been done for μ decay, from the results of only five key experiments. These five τ decay experiments would determine upper limits for all eighteen non-$(V-A)$ terms and a lower limit for the $V-A$ coupling. Most of these experiments can be carried out at an e^+e^- collider with unpolarized beams near τ pair production threshold as well as in the region of the Υ resonances. Analytical decay distributions are derived in terms of suitable laboratory observables. With their help statistical errors for the decay parameters ρ_e, η_e, δ_e, ξ_e, ρ_μ, η_μ, δ_μ, ξ_μ, ξ_π, and ξ_K are calculated assuming an ideal detector. For 10^7 produced $\tau^+\tau^-$ pairs these errors are in the range of $(2-20)\times 10^{-3}$ except the error for η_e ($\Delta\eta_e = 0.53$). The parameters ρ and η that describe the isotropic part of the spectrum are found to be strongly correlated. Therefore any experiment should be analyzed simultaneously with respect to both parameters. An experimental value of η_μ is required for the derivation of the Fermi coupling constant for the muonic decay. By measuring the μ^+ polarization from τ^+ decay the polarization parameter ξ'_μ can be deduced with an error of 15%. The measurements of ξ_e and δ_e will allow us to constrain five of the ten complex coupling constants for the decay $\tau^+ \to e^+ \nu_e \bar{\nu}_\tau$, the measurements of ξ_μ, δ_μ, and ξ'_μ will even constrain eight complex coupling constants for the decay $\tau^+ \to \mu^+ \nu_\mu \bar{\nu}_\tau$. The determination of the remaining coupling constants would require the measurement of the cross section for the inverse decay $\nu_\tau e^- \to \tau^- \nu_e$ or of correlations between one of the neutrinos and the μ^+ or τ^+ for the muonic decay.

I. INTRODUCTION

Leptonic decays of heavy leptons are especially well suited to investigate the structure of the charged weak interaction. The classical example is the muon, where it has recently been shown that the Lorentz structure of the interaction can be determined entirely from experiments without specific model assumptions.[1] This analysis established the $V-A$ coupling as being dominant, and set upper limits for the remaining nine couplings. The τ lepton, with its two leptonic decays $\tau \to \mu \bar{\nu}_\mu \nu_\tau$ and $\tau \to e \bar{\nu}_e \nu_\tau$, gives us a unique opportunity to study the universality of the charged leptonic weak interaction. To be more specific: Are these two decays just duplicates of μ decay, governed by the same type of weak interaction, i.e., $V-A$? As in μ decay there is a choice of ten different complex couplings corresponding to nineteen coupling constants to be determined by experiment. In an appropriate representation $V-A$ corresponds to only one real coupling constant. As has been done for μ decay, the $V-A$ hypothesis can be proven experimentally by measuring the decay probability and four additional parameters yielding information about the lepton chiralities. These would determine upper limits for all eighteen non-$(V-A)$ terms and a lower limit for the $V-A$ coupling. Most of these experiments can be carried out also for the two decays $\tau^+ \to \mu^+ \nu_\mu \bar{\nu}_\tau$ and $\tau^+ \to e^+ \nu_e \bar{\nu}_\tau$, although the methods are somewhat different due to the short τ lifetime. For τ decays, the important asymmetry parameters ξ and δ (and also the spectral shape parameters ρ and η) can be measured efficiently by taking into account the spin correlation of the τ^+ and τ^- produced in e^+e^- collisions. Therefore we derive analytical expressions for spin-correlated $\tau^+\tau^-$ decay distributions in terms of appropriate laboratory variables. The polarization parameter ξ'_μ for μ^+ from τ^+ decay can be measured by detecting the decay asymmetry of the μ^+; here we calculate the polarization ζ_μ of the μ in the laboratory system. The low-energy parameter η_μ, finally, is important as a correction to the Fermi coupling constant G_F.[2] It can be measured directly, as mentioned above, but it is also constrained by the values of ξ_μ, δ_μ, and ξ'_μ. In summary the proposed experiments allow us to derive upper limits to five of the ten complex coupling constants for the decay $\tau^+ \to e^+ \nu_e \bar{\nu}_\tau$ and to eight coupling constants for the decay $\tau^+ \to \mu^+ \nu_\mu \bar{\nu}_\tau$; the difference being due to the knowledge of the μ^+ polarization ξ'_μ. The determination of the remaining coupling constants would require the measurement of the cross section for the inverse decay $\nu_\tau e^- \to \tau^- \nu_e$ or of correlations between one of the neutrinos and the μ^+ or τ^+ for the muonic decay.

II. μ DECAY

A. Muon-decay interaction

The universality of the charged weak interaction allows us to describe on the same basis such a wide range of phenomena as nuclear β decay, muon decay, and semileptonic decays of hadrons. This is incorporated by the standard model[3] which is characterized by left-handed fermions $(V-A)$ and by the universal Fermi coupling constant G_F.

The experimental investigation of the charged weak interaction is especially rewarding in the case of leptonic decays of heavy leptons where one is not hampered by the strong interaction. Thus, for example, the Fermi coupling constant is deduced from muon decay assuming a $V-A$ interaction. The experimental verification of this assumption, however, was found only recently[1] by the author, Gerber, and Johnson. Their analysis, moreover, allows us to derive upper limits for all of the other nine possible couplings, valid independent of specific models. The method used there can readily be applied to the two decays $\tau\to\mu\bar{\nu}_\mu\nu_\tau$ and $\tau\to e\bar{\nu}_e\nu_\tau$ as well.

Leptonic decays can be described by the most general, local, derivative-free and lepton-number-conserving four-fermion point-interaction Hamiltonian.[4] It contains ten complex coupling constants corresponding to 19 independent parameters to be determined by experiment. The observables are described most conveniently in terms of a Hamiltonian in charge changing and "helicity projection" form[5,6] which is characterized by fields of definite handedness. The matrix element for μ decay is given by[1]

$$M=4\frac{G_F}{\sqrt{2}}\sum_{\substack{\gamma=S,V,T\\ \epsilon,\mu=R,L}} g^{\gamma}_{\epsilon\mu}\langle\overline{e_\epsilon}|\Gamma^\gamma|(\nu_e)_n\rangle\langle(\overline{\nu_\mu})_m|\Gamma_\gamma|\mu_\mu\rangle\ . \tag{2.1}$$

γ labels the type of interaction: $\Gamma^S,\Gamma^V,\Gamma^T$ (scalar, vector, tensor). The indices ϵ and μ indicate the chiral projection (left-handed, right-handed) of the spinors of the experimentally observed particles, $\epsilon\hat{=}$electron, $\mu\hat{=}$muon. The helicities n and m for the ν_e and the ν_μ, respectively, are uniquely determined for given γ,ϵ,μ. In this picture, the standard model corresponds to $g^V_{LL}=1$, all other couplings being zero.

The strength of the interaction is determined by the μ lifetime. Since we are only interested in the relative weights of the different couplings, the $g^\gamma_{\epsilon\mu}$ are normalized:

$$\begin{aligned}A\equiv{}&4(|g^S_{RR}|^2+|g^S_{LR}|^2+|g^2_{RL}|^2+|g^S_{LL}|^2)\\&+16(|g^V_{RR}|^2+|g^V_{LR}|^2+|g^V_{RL}|^2+|g^V_{LL}|^2)\\&+48(|g^T_{LR}|^2+|g^T_{RL}|^2):=16\ .\end{aligned}\tag{2.2}$$

This allows us to define the four probabilities $Q_{\epsilon\mu}$ of obtaining an electron of handedness ϵ from a muon of handedness μ in μ decay:

$$Q_{RR}\equiv\tfrac{1}{4}|g^S_{RR}|^2+|g^V_{RR}|^2=2(b+b')/A\ , \tag{2.3}$$

$$\begin{aligned}Q_{LR}\equiv{}&\tfrac{1}{4}|g^S_{LR}|^2+|g^V_{LR}|^2+3|g^T_{LR}|^2\\&=[(a-a')+6(c-c')]/2A\ ,\end{aligned}\tag{2.4}$$

$$\begin{aligned}Q_{RL}\equiv{}&\tfrac{1}{4}|g^S_{RL}|^2+|g^V_{RL}|^2+3|g^T_{RL}|^2\\&=[(a+a')+6(c+c')]/2A\ ,\end{aligned}\tag{2.5}$$

$$Q_{LL}\equiv\tfrac{1}{4}|g^S_{LL}|^2+|g^V_{LL}|^2=2(b-b')/A\ . \tag{2.6}$$

We note that $0\le Q_{\epsilon\mu}\le 1$ and $\sum_{\epsilon,\mu}Q_{\epsilon\mu}=1$. The parameters $\{a/A,\ldots,c'/A\}$ have been introduced[7] to express all possible results of the measurements on the positron in the decay of polarized (and unpolarized) muons. Their values have been derived for muon decay[1,8] from the following, complete set of measurements.

(i) Shape of positron energy spectrum,[9]

$$\rho=0.752\pm0.0027\ .$$

(ii) Decay asymmetry between μ spin and e momentum at spectrum end point,[10]

$$\xi\delta/\rho=0.9989\pm0.0023\ .$$

(iii) Differential decay asymmetry,[11]

$$\delta=0.7502\pm0.0043\ .$$

The polarization vector (P_L,P_{T_1},P_{T_2}) of the positron yields the remaining six parameters.

(iv) Longitudinal polarization,[12]

$$\langle P_L\rangle\equiv\xi'=0.998\pm0.045\ .$$

(v) Angular dependence of P_L,[12]

$$\xi''=0.65\pm0.36\ .$$

(vi) and (vii) Energy dependence of P_{T_1},

$$\alpha/A=0.015\pm0.052\ ,$$

$$\beta/A=0.002\pm0.018\ .$$

(viii) and (ix) Energy dependence of P_{T_2},[8]

$$\alpha'/A=-0.047\pm0.052\ ,$$

$$\beta'/A=0.017\pm0.018\ .$$

One finds upper limits for Q_{RR}, Q_{LR}, and Q_{RL}, which in turn yield upper limits for the absolute values of eight complex coupling constants $g^\gamma_{\epsilon\mu}$. Since Q_{LL} is bounded by a lower limit, it is not possible to deduce an upper limit for $|g^S_{LL}|$ from normal muon decay without detecting the neutrinos. In fact, with the data from normal muon decay we cannot tell if

$$g^S_{LL}=0,\quad g^V_{LL}=1\quad(V-A)\ ,$$

or

$$g^S_{LL}=2,\quad g^V_{LL}=0\ .$$

This kind of ambiguity has been noted by Jarlskog[13] in the context of a different form of the Hamiltonian. She proposed to measure electron-neutrino correlations to resolve it, experiments which have not been performed to date. It has, however, been pointed out[1] that the information from inverse muon decay allows us to resolve this ambiguity:

$$\nu_\mu + e^- \rightarrow \mu^- + \nu_e \ .$$

The total rate S, normalized to the rate predicted by $V-A$, is found to be $S=0.98\pm0.12$.[14] S has been calculated in terms of the charge changing Hamiltonian in the parity representation.[15] In terms of our $g^\gamma_{e\mu}$ (helicity representation) one gets

$$S=\tfrac{1}{2}(1-h)(|g^V_{LL}|^2+\tfrac{3}{8}|g^V_{RL}|^2+\tfrac{3}{32}|g^S_{LR}-\tfrac{10}{3}g^T_{LR}|^2+\tfrac{3}{32}|g^S_{RR}|^2+\tfrac{4}{3}|g^T_{LR}|^2)$$
$$+\tfrac{1}{2}(1+h)(|g^V_{RR}|^2+\tfrac{3}{8}|g^V_{LR}|^2+\tfrac{3}{32}|g^S_{RL}-\tfrac{10}{3}g^T_{RL}|^2+\tfrac{3}{32}|g^S_{LL}|^2+\tfrac{4}{3}|g^T_{RL}|^2) \ , \tag{2.7}$$

where h is the helicity of the ν_μ from pion decay. The deviation of $|h|$ from 1 is known very precisely: $1-|h|<4.1\times10^{-3}$;[16,10] the sign of h has been determined by *electromagnetic* interaction for ν_μ and $\bar{\nu}_\mu$.[17,18] Thus S gives information about the first 5 coupling constants g^V_{LL}, g^V_{RL}, g^S_{LR}, g^T_{LR}, and g^S_{RR}, all of which couple to left-handed ν_μ. The influence of four of them on S is found to be negligible with the upper limits derived from *normal* muon decay. One obtains

$$S=|g^V_{LL}|^2 \ ,$$

which yields a *lower* limit for $|g^V_{LL}|$, and through the normalization requirement one gets an upper limit for the remaining $|g^S_{LL}|$:

$$|g^S_{LL}|^2<4(1-S) \ .$$

Thus the weak interaction has been completely determined between the electron and the muon and their neutrinos in normal and inverse muon decay using only *leptonic* data. The results are shown in Fig. 1, where each of the ten coupling constants is given within one of the squares defined uniquely by the handednesses of electron and muon and by the type of interaction. The outer circles display the mathematical limits for the $g^\gamma_{\epsilon\mu}$ in the complex plane, the inner circles for nine of the $g^\gamma_{\epsilon\mu}$ show the areas still allowed by experiment (90% c.l.). For g^V_{LL}, which has been chosen to be real, one gets the small line close to $g^V_{LL}=1$ in agreement with $V-A$.

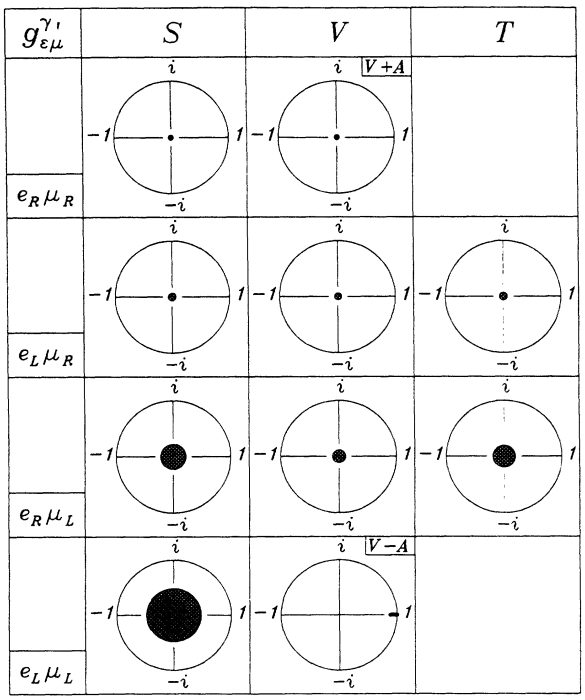

FIG. 1. 90%-C.L. limits (Ref. 1) for the reduced coupling constants $g^\gamma_{\epsilon\mu}/\max(g^\gamma_{\epsilon\mu})$ for the decay $\mu^- \rightarrow e^- \bar{\nu}_e \nu_\mu$. Each coupling is uniquely determined by the handednesses ϵ and μ of the electron and the muon, respectively, and the type of interaction $\gamma=S$, V, or T. The maximal possible values $\max(g^\gamma_{\epsilon\mu})$ of the coupling constants are 2, 1, and $1/\sqrt{3}$ for $\gamma=S$, V, and T, respectively.

B. Key experiments

We have seen in muon decay that it is not necessary to perform all of the 19 possible measurements in order to determine the interaction. The standard model predicts $V-A$ corresponding to $g^V_{LL}=1$. We can then find a minimal set of measurements needed to *prove* this hypothesis by experiment by calculating the probability $P^e_R \equiv Q_{RR}+Q_{RL}$ to obtain a right-handed electron and $P^\mu_R \equiv Q_{RR}+Q_{LR}$ for a right-handed muon:[19]

$$P^e_R=\tfrac{1}{4}|g^S_{RR}|^2+\tfrac{1}{4}|g^S_{RL}|^2+|g^V_{RR}|^2+|g^V_{RL}|^2$$
$$+3|g^T_{RL}|^2=\tfrac{1}{2}(1-\xi') \ , \tag{2.8}$$

$$P^\mu_R=\tfrac{1}{4}|g^S_{RR}|^2+\tfrac{1}{4}|g^S_{LR}|^2+|g^V_{RR}|^2+|g^V_{LR}|^2$$
$$+3|g^T_{LR}|^2=\tfrac{1}{2}[1+\tfrac{1}{9}(3\xi-16\xi\delta)] \ . \tag{2.9}$$

By measuring the positron polarization ξ' one obtains upper limits for five complex coupling constants, by measuring the decay asymmetry three additional ones. We can conclude that if the standard-model hypothesis is correct, then only the following five experiments are necessary to determine the interaction: τ_μ ($\rightarrow$Fermi coupling constant), δ, ξ, and ξ' ($\rightarrow$16 decay parameters), and $S(\nu_\mu+e^- \rightarrow \mu^-+\nu_e)$ ($\rightarrow V-A$).

III. τ DECAY

Leptonic τ decays are described by the same Hamiltonian as μ decay. They are insensitive to effects of the finite mass of the intermediate vector boson, since the lifetime and the decay parameters are modified by terms of the order of $(m_\tau/m_W)^2 \approx 0.5\times 10^{-3}$.[20] Effects of a finite τ-neutrino mass m_{ν_τ} are in the order of $\sigma = m_{\nu_\tau}^2/m_\tau^2$.[21] With the present experimental limit of 35 MeV/c^2 (Ref. 22) any possible effect is $\lesssim 0.4\times 10^{-3}$. The effects of radiative corrections, however, do have to be taken into account[23] when analyzing a real experiment, but they can be neglected in this context where we try to derive the magnitude of the errors in a future experiment.

A. Universality of the interaction

The universality of the charged weak interaction for the three decays

$$\mu\to\nu_\mu e\bar{\nu}_e,\quad \tau\to\nu_\tau\mu\bar{\nu}_\mu \text{ and } \tau\to\nu_e e\bar{\nu}_e$$

can be checked by testing if (a) the couplings are equal and (b) the strength is the same. The Fermi coupling constant is given by[2]

$$G_F^2=\frac{1}{\tau_l}\frac{192\pi^3}{m_l^5}\frac{1}{1+4\eta m_{l'}/m_l}\ , \tag{3.1}$$

where τ_l is the lifetime of the mother lepton l, m_l its mass and m_l' the mass of the charged daughter lepton. Higher-order corrections have been neglected here. η is the low-energy spectrum parameter. It is important for the muonic decay of the τ,[24] since $m_\mu/m_\tau \approx \frac{1}{17}$. With $|\eta_\mu|\le 1$ this gives a relative error $\Delta G_F/G_F \le 12\%$. η can be determined (a) by analyzing the muon momentum distribution (see Sec. VI) and (b) by deriving upper limits for the coupling constants by measuring ξ'_μ, ξ_μ, and δ_μ [see Eqs. (2.8), (2.9), and Sec. VI]. The upper limits thus obtained for the coupling constants constrain the value of η according to Eq. (3.4).

B. Spectrum shape: Scalar observables

1. *Michel parameter* ρ

This is the only decay parameter measured up to date.[25] Although it is not one of the key experiments, it would be very exciting if $\rho\neq\frac{3}{4}$ as has been discussed elsewhere.[26] If $\rho=\frac{3}{4}$, we do not learn very much: Any combination of the six couplings $g_{LL}^S, g_{LR}^S, g_{RL}^S, g_{RR}^S, g_{RR}^V, g_{LL}^V$ with the other four couplings being zero yields $\rho=\frac{3}{4}$. This can be seen from

$$\rho=\tfrac{3}{4}-\tfrac{3}{4}[|g_{LR}^V|^2+|g_{RL}^V|^2+2|g_{LR}^T|^2+2|g_{RL}^T|^2 + \mathrm{Re}(g_{LR}^S g_{LR}^{T*}+g_{RL}^S g_{RL}^{T*})]\ , \tag{3.2}$$

$$\rho=\tfrac{3}{4}\Longrightarrow(|g_{LR}^V|^2+|g_{RL}^V|^2+2|g_{LR}^T|^2+2|g_{RL}^T|^2) = -\mathrm{Re}(g_{LR}^S g_{LR}^{T*}+g_{RL}^S g_{RL}^{T*})\ . \tag{3.3}$$

For $g_{LR}^T=g_{RL}^T=0$ we find $g_{LR}^V=g_{RL}^V=0$, with all other couplings being arbitrary.

We note especially that $V+A$ cannot be excluded if ρ is found to be $\frac{3}{4}$. There are three possible contributions:

$$(\alpha)\ g_{RL}^V:\ \begin{cases}\text{coupling to RH } \mu\ ,\\ \text{coupling to LH } \tau\ ,\end{cases}$$

$$(\beta)\ g_{LR}^V:\ \begin{cases}\text{coupling to LH } \mu\ ,\\ \text{coupling to RH } \tau\ ,\end{cases}$$

$$(\gamma)\ g_{RR}^V:\ \begin{cases}\text{coupling to RH } \mu\ ,\\ \text{coupling to RH } \tau\ .\end{cases}$$

As seen above $\rho=\frac{3}{4}$ excludes g_{RL}^V and g_{LR}^V [$\hat{=}$mixing of right-handed (RH) and left-handed (LH) currents] only if there are no simultaneous scalar and tensor couplings. The pure right-handed coupling g_{RR}^V, however, is always possible.

2. *Low-energy parameter* η

Although η is not a restrictive parameter, its value is needed to derive the Fermi coupling constant. In terms of our $g_{\epsilon\mu}^\gamma$,

$$\eta=\tfrac{1}{2}\mathrm{Re}(6g_{RL}^V g_{LR}^{T*}+6g_{LR}^V g_{RL}^{T*}+g_{RR}^S g_{LL}^{V*} + g_{RL}^S g_{LR}^{V*}+g_{LR}^S g_{RL}^{V*}+g_{LL}^S g_{RR}^{V*})\ . \tag{3.4}$$

Thus $\eta\neq 0$ shows there are at least two different couplings with opposite chiralities for the charged leptons which would result in *nonmaximal* parity and charge-conjugation violation.

In this case if we assume $V-A$ (g_{LL}^V) to be dominant, then the second coupling would be a Higgs-type coupling (g_{RR}^S) with right-handed τ and μ.

C. Lepton chiralities: pseudoscalar observables

We emphasize again the importance of the pseudoscalar observables. As mentioned earlier, the key experiments in leptonic decays consist of determining the chiralities of three of the four involved leptons. For muon decay all of the necessary experiments have been performed: (1) for the muon (positron decay asymmetry for polarized muons described by ξ and δ), (2) for the electron (longitudinal polarization ξ'), (3) for the muon neutrino (cross section S for inverse muon decay with ν_μ of negative helicity). The first two of these can also be done for leptonic τ decays, though the methods are somewhat different due to the short τ lifetime.

The polarization of the μ^+ from τ^+ decay can be analyzed by measuring the decay symmetry of the stopped muons.[24] The analyzing power is $\frac{1}{3}$ and has been measured with a precision of $<1\%$.[27]

The decay asymmetry of the positrons from muon decay is measured by stopping polarized muons and detecting the decay positrons as a function of the emission angle relative to the muon polarization. In τ decay it is not possible at present to measure the direction and polarization of the τ.

One can, however, get information about the τ polar-

ization by making use of the spin correlation of the two τ's.[28] Because of the Lorentz boost the momentum correlation function of the two observed leptons contains information about the c.m. angles and therefore also about the decay asymmetry. This dependence is, however, rather weak and vanishes at the threshold of τ pair production.

We have proposed to use as observables the momenta of the two charged particles from τ^+ and τ^- decay and the opening angle θ_{34} between these momenta.[24] It will be shown in Sec. VI that the corresponding correlation functions are much more sensitive to ξ and δ than the momentum correlation function, and retain some of their sensitivity at τ-pair threshold.

D. Neutrino helicity and sign of the parity violation

As the method described in the previous section yields only the absolute values of the parity-violating quantities ξ_μ, ξ_e, and $\xi_\pi = h_{\nu_\tau}$, it is still necessary to determine their sign. The determination of the sign of one of them, say, h_{ν_τ}, fixes the sign of the remaining ones. Instead of using longitudinally polarized e^+ and e^- beams, we propose to use the method of Kühn and Wagner,[29] with the strong decay of the $a_1(1270)$ meson as analyzer. The analyzing power for this process is in the order of a few percent, sufficient to determine h_{ν_τ} a few standard deviations from zero, and thus the *sign* of h_{ν_τ}. The correlation experiment between μ, e, and π would yield the absolute value of h_{ν_τ} with high precision.

IV. DECAY DISTRIBUTIONS OF SPIN-CORRELATED τ PAIRS

A. Introduction

Distribution functions for the decay of spin-correlated heavy lepton pairs from e^+e^- collisions have been calculated by Tsai[28] assuming the heavy leptons to decay via a $V-A$ interaction. The motivation was to find a signature which would allow us to find and identify the presumed heavy lepton. Shortly after the discovery of the τ lepton[30] these calculations were generalized by Pi and Sanda[31] to polarized e^+, e^- beams and to τ decay spectra with arbitrary decay parameters ρ, δ, ξ, and η. Their distribution functions are given in terms of c.m. variables which are not accessible to direct measurement, since the τ's are not detected. They also show how various laboratory observables depend on the type of interaction in leptonic τ decays. Although this is very instructive, it does not allow us to calculate any limits for the decay parameters or coupling constants for a given amount of events.

We make use of a quite different approach. Our aim is to determine the Lorentz structure by obtaining experimental limits to the coupling constants $g^\gamma_{\epsilon\mu}$. This can be achieved by choosing an appropriate set of the decay parameters as described in Secs. II and III. Here we derive the formulas which allow us to deduce errors of the decay parameters for a given number of events.

With this motivation in mind we restrict some of the generality of Pi and Sanda's distributions there, where it would not matter. Thus we use only the cross sections for unpolarized beams, since this is sufficient to measure also the parity-violating parameters ξ and δ. We keep the full generality, however, for the decay spectrum with the ambition to measure as many of the decay parameters as possible. We further use normalized decay distributions, thus separating off the $\tau^+\tau^-$ production probability in which we are not interested here.

We have found a set of laboratory variables which retains much of the angular information of the c.m. system needed to determine ξ and δ.[24] It consists of the momenta k_3 and k_4 of the detected particles and the opening angle θ_{34} between them. The distributions of Pi and Sanda have been transformed to these variables and integrated analytically over unobservable quantities assuming a detector with 100% solid angle efficiency. A real, generally cylindrical detector will yield slightly different results, but the changes will be predominantly quantitative, enlarging the statistical error by, say, 50%. Cuts on the momenta, however, are possible and straightforward, since the distributions depend directly on them.

B. Notation

We regard the production process

$$e^+e^- \to \tau^+\tau^-$$

and the subsequent decay processes

$$\tau^+ \to \begin{cases} (e^+\nu_e)\bar{\nu}_\tau , \\ (\mu^+\nu_\mu)\bar{\nu}_\tau , \\ \pi^+\bar{\nu}_\tau , \\ K^+\bar{\nu}_\tau , \end{cases}$$

$$\tau^- \to \begin{cases} (e^-\bar{\nu}_e)\nu_\tau , \\ (\mu^-\bar{\nu}_\mu)\nu_\tau , \\ \pi^-\nu_\tau , \\ K^-\nu_\tau . \end{cases}$$

The τ leptons and their charged decay products are labeled by numbers:

particle $1 \equiv \tau^+$,

particle $2 \equiv \tau^-$,

particle $3 \equiv e^+, \mu^+, \pi^+,$ or K^+ ,

particle $4 \equiv e^-, \mu^-, \pi^-,$ or K^- ,

where any combination of particle 3 and 4 is allowed. Variables measured in the rest systems of particles 1 and 2, respectively, are designated by an asterisk.

E_0 is the total energy of the system, $E_1 = E_0/2$ is the incident c.m. energy, m_1 the mass of the τ lepton, and $\gamma = E_1/m_1 = (1-\beta^2)^{-1/2}$. We use three frames in the

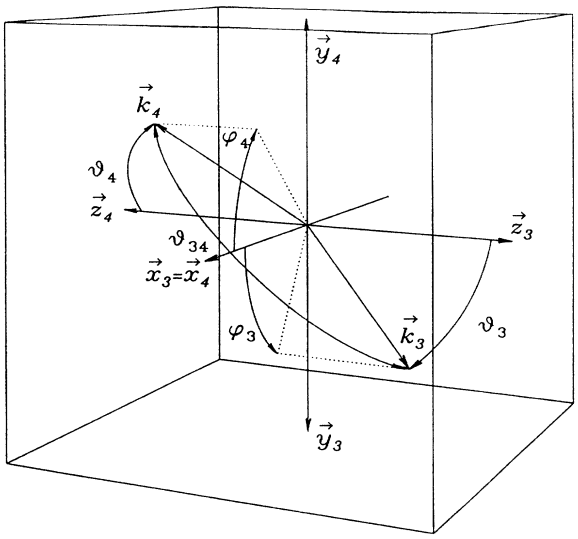

FIG. 2. Coordinate systems for the decay of correlated $\tau^+\tau^-$ pairs. $\hat{\mathbf{z}}_3$ and $\hat{\mathbf{z}}_4$ are the directions of the τ^+ and τ^-, respectively, while $\mathbf{k}_3$ and $\mathbf{k}_4$ are the momenta of their corresponding charged decay products with spherical coordinates (k_3,ϕ_3,θ_3) and (k_4,ϕ_4,θ_4).

laboratory system: The first frame describes the τ pair production, with the z axis pointing in the positron beam direction. The τ^+ is then emitted under the polar angle θ_1. We need not specify an azimuthal angle ϕ_1, since we disregard effects of transverse beam polarization.

The z axes of the second and third coordinate system point in the direction of the τ^+ and τ^-, respectively. Thus the momentum variables k_3, θ_3, ϕ_3 $(d^3k_3=k_3^2dk_3d\cos\theta_3d\phi_3)$ are defined relative to $\mathbf{k}_1$, the variables k_4, θ_4, ϕ_4 $(d^3k_4=k_4^2dk_4d\cos\theta_4d\phi_4)$ relative to $\mathbf{k}_2=-\mathbf{k}_1$ (see Fig. 2). Here again we need not specify a specific x axis; we only demand the axes $\hat{\mathbf{x}}_3$ and $\hat{\mathbf{x}}_4$ to coincide and note that $\hat{\mathbf{y}}_3=-\hat{\mathbf{y}}_4$, $\hat{\mathbf{z}}_3=-\hat{\mathbf{z}}_4$.

C. Normalized decay distributions

1. General form of single particle distribution

The normalized decay distributions for a $\tau^\pm$ with polarization vector $\boldsymbol{\zeta}$ in the τ rest system are given by

$$\frac{d^3W^+}{d^3k_3^*}=[G_1^{(3)}+\xi_3(\boldsymbol{\zeta}\cdot\mathbf{k}_3^*)G_2^{(3)}] \tag{4.1}$$

and

$$\frac{d^3W^-}{d^3k_4^*}=[G_1^{(4)}-\xi_4(\boldsymbol{\zeta}\cdot\mathbf{k}_4^*)G_2^{(4)}] \tag{4.2}$$

with

$$\xi_3=\begin{cases}\xi_e,\xi_\mu & \text{for } \mu^+,e^+ ,\\ -h_{\bar{\nu}_r} & \text{for } \pi^+,K^+ ,\end{cases}$$

$$\xi_4=\begin{cases}\xi_e,\xi_\mu & \text{for } \mu^-,e^- ,\\ +h_{\nu_r} & \text{for } \pi^-,K^- ,\end{cases}$$

where h designs the helicity of the $\bar{\nu}_\tau$ (ν_τ). For a $V-A$ interaction $\xi_e=\xi_\mu=+1$, $\xi_\pi=\xi_K=-1$.

2. Leptonic decay distribution

The leptonic decay distribution is given by[2]

$$\begin{aligned}G_1^{(i)}&=\frac{1}{4\pi\lambda_iE_i^*}(a_0^{(i)}+a_1^{(i)}E_i^*+a_2^{(i)}E_i^{*2})\\&\equiv\frac{g_1^{(i)}}{4\pi\lambda_iE_i^*} ,\\ G_2^{(i)}&=\frac{1}{4\pi\lambda_iE_i^*}(b_0^{(i)}+b_1^{(i)}E_i^*)\equiv\frac{g_2^{(i)}}{4\pi\lambda_iE_i^*}\end{aligned} \tag{4.3}$$

with

$$\begin{aligned}a_0^{(i)}&=-\tfrac{2}{9}\rho_im_i^2+\eta_im_iW_i ,\\ b_0^{(i)}&=\tfrac{1}{9}(3-8\delta_i)W_i+\tfrac{2}{9}\delta_iP_i ,\\ a_1^{(i)}&=(1-\tfrac{2}{3}\rho_i)W_i-\eta_im_i ,\\ b_1^{(i)}&=\tfrac{1}{9}(8\delta_i-3) ,\\ a_2^{(i)}&=(\tfrac{8}{9}\rho_i-1) .\end{aligned} \tag{4.4}$$

ρ_i, η_i, δ_i, and ξ_i are the leptonic decay parameters, their $V-A$ values being $\rho_i=\frac{3}{4}$, $\eta_i=0$, $\delta_i=\frac{3}{4}$, $\xi_i=1$. The maximal energy of the daughter leptons in the τ rest system is given by

$$W_i=\frac{m_1^2+m_i^2}{2m_1} ,$$

the corresponding momentum by

$$P_i=\frac{m_1^2-m_i^2}{2m_1} ,$$

and λ_i is a normalization factor:

$$\begin{aligned}\lambda_i&=\int_{m_i}^{W_i}\frac{a_0^{(i)}+a_1^{(i)}E_i^*+a_2^{(i)}E_i^{*2}}{E_i^*}k_i^{*2}dk_i^*\\&=\left[\tfrac{1}{12}P_i^3W_i-\tfrac{1}{8}m_i^2P_iW_i+\tfrac{1}{8}m_i^4\ln\frac{W_i+P_i}{m_i}\right]\\&\quad+\eta_im_i\left[-\tfrac{1}{3}P_i^3+\tfrac{1}{2}P_iW_i^2-\tfrac{1}{2}m_i^2W_i\ln\frac{W_i+P_i}{m_i}\right] .\end{aligned} \tag{4.5}$$

3. Semileptonic decay distribution

$$G_1^{(i)}=G_2^{(i)}=\frac{1}{4\pi\lambda_i}\frac{\delta(k_4^*-P_4)}{P_4^2} \tag{4.6}$$

with

$$\lambda_i=1$$

or, as a function of $\cos\theta_4$,

$$G_1^{(i)}=G_2^{(i)}=\frac{1}{4\pi\beta\gamma}\frac{\delta(\cos\theta_4-\cos\zeta_4)}{k_4P_4W_4}\ , \tag{4.7}$$

where ζ_4 is the angle of emission of the pseudoscalar meson (see Sec. IV C 5).

4. Normalized correlated distribution for unpolarized beams

The correlated distribution for unpolarized beams[31] is used in the following, normalized form:

$$\begin{aligned}\frac{d^8\sigma}{d^3k_3^*d^3k_4^*d\Omega_1}=\frac{3}{8\pi}\frac{\gamma^2}{2\gamma^2+1}\Bigg\{&G_1^{(3)}G_1^{(4)}\left[1+\cos^2\theta_1+\frac{\sin^2\theta_1}{\gamma^2}\right]\\&+\xi_3\xi_4k_3^*k_4^*G_2^{(3)}G_2^{(4)}\Bigg[\cos\theta_3^*\cos\theta_4^*\left[1+\cos^2\theta_1-\frac{\sin^2\theta_1}{\gamma^2}\right]\\&+\sin\theta_3^*\sin\phi_3^*\sin\theta_4^*\sin\phi_4^*\left[1-\frac{1}{\gamma^2}\right]\sin^2\theta_1\\&-\sin\theta_3^*\cos\phi_3^*\sin\theta_4^*\cos\phi_4^*\left[1+\frac{1}{\gamma^2}\right]\sin^2\theta_1\\&+(\cos\theta_3^*\sin\theta_4^*\cos\phi_4^*-\sin\theta_3^*\cos\phi_3^*\cos\theta_4^*)\frac{1}{\gamma}\sin2\theta_1\Bigg]\Bigg\}\ .\end{aligned} \tag{4.8}$$

5. Some useful relations

(a) Lorentz transformation

$$k_i^*\sin\theta_i^*=k_i\sin\theta_1,\quad E_i^*=\gamma(E_i-\beta k_i\cos\theta_i),\quad k_i^*\cos\theta_i^*=\gamma(k_i\cos\theta_i-\beta E_i),\quad \phi_i^*=\phi_i\ . \tag{4.9}$$

(b) Jacobian

$$\frac{\partial(k_i^*,\cos\theta_i^*)}{\partial(k_i,\cos\theta_i)}=\frac{E_i^*}{k_i^{*2}}\frac{k_i^2}{E_i}\ . \tag{4.10}$$

(c) Angular range

$$\text{Mesons: } \theta_i=\zeta_i,\quad \text{Leptons: } 0\le\theta_i\le\zeta_i \tag{4.11}$$

with

$$\zeta_i=\begin{cases}\arccos\left[\dfrac{\gamma E_i-W_i}{\beta\gamma k_i}\right] & \text{for } k_i\ge\gamma(P_i-\beta W_i)\ ,\\ 180^\circ \text{ for } k_i<\gamma(P_i-\beta W_i)\ .\end{cases} \tag{4.12}$$

6. Normalized distribution in the laboratory system

$$\frac{d^5\sigma}{dk_3dk_4d\cos\theta_{34}d\Omega_1}=\int\left[\frac{d^8\sigma k_3^{*2}k_4^{*2}}{d^3k_3^*d^3k_4^*d\Omega_1}\right]\left|\frac{\partial(k_3^*,\cos\theta_3^*)}{\partial(k_3,\cos\theta_3)}\right|\left|\frac{\partial(k_4^*,\cos\theta_4^*)}{\partial(k_3,\cos\theta_4)}\right|\left|\frac{\partial\phi_4}{\partial\cos\theta_{34}}\right|d\phi_3d\cos\theta_3d\cos\theta_4\ . \tag{4.13}$$

After averaging over the τ direction and integrating over the azimuthal angle ϕ_3 one obtains the general normalized distribution

$$\frac{d^3\sigma}{dk_3dk_4d\cos\theta_{34}}=4\pi\frac{k_3^2k_4^2}{E_3E_4}\int\frac{E_3^*E_4^*}{Q}d\cos\theta_3d\cos\theta_4\{G_1^{(3)}G_1^{(4)}+\xi_3\xi_4G_2^{(3)}G_2^{(4)}[(k_3^*\cos\theta_3^*)(k_4^*\cos\theta_4^*)u_1 + k_3k_4(\cos\theta_{34}+\cos\theta_3\cos\theta_4)u_2]\} \quad (4.14)$$

with

$$Q=\sqrt{\sin^2\theta_3\sin^2\theta_4-(\cos\theta_{34}+\cos\theta_3\cos\theta_4)^2},\quad u_1=\frac{2\gamma^2-1}{2\gamma^2+1},\quad u_2=\frac{1}{2\gamma^2+1}\ .$$

The c.m. expressions E_i^* and $k_i^*\cos\theta_i^*$ are given in Eq. (4.9) in terms of the laboratory variables k_i and $\cos\theta_i$.

D. Momentum-momentum angular distributions

1. Lepton-lepton correlations

For lepton-lepton-correlations the integration of Eq. (4.14) has to be performed over an area specified by the momenta k_3 and k_4 and the opening angle θ_{34} (see the Appendix).

The normalized distribution function $R=d^3\sigma/dk_3dk_4d\cos\theta_{34}$ can then be written as

$$R(k_3,k_4,\cos\theta_{34})=\frac{1}{4\pi\lambda_3\lambda_4}\frac{k_3^2k_4^2}{E_3E_4}\{F_0(k_3,k_4,\cos\theta_{34})+\xi_3\xi_4[F_1(k_3,k_4,\cos\theta_{34})u_1(\gamma)+F_2(k_3,k_4,\cos\theta_{34})u_2(\gamma)]\} \quad (4.15)$$

with

$$u_1(\gamma)=\frac{2\gamma^2-1}{2\gamma^2+1},\quad u_2(\gamma)=\frac{1}{2\gamma^2+1}\ .$$

The functions F_0, F_1, and F_2 can be factorized into terms $A_\mu^{(i)}$, $B_\mu^{(i)}$, and $C_\mu^{(i)}$ which depend only on the momentum k_i and on the decay parameters, but not on $\cos\theta_{34}$, and into the integrals $M_{\mu\nu}$ which depend on all three variables k_3, k_4, and $\cos\theta_{34}$:

$$F_0(k_3,k_4,\cos\theta_{34})=\int g_1^{(3)}g_1^{(4)}\frac{d\cos\theta_3d\cos\theta_4}{Q}=\sum_{\mu,\nu=0}^{2}A_\mu^{(3)}(k_3)A_\nu^{(4)}(k_4)M_{\mu\nu}(k_3,k_4,\cos\theta_{34})\ , \quad (4.16)$$

$$F_1(k_3,k_4,\cos\theta_{34})=\int(g_2^{(3)}k_3^*\cos\theta_3^*)(g_2^{(4)}k_4^*\cos\theta_4^*)\frac{d\cos\theta_3d\cos\theta_4}{Q}=\sum_{\mu,\nu=0}^{2}B_\mu^{(3)}(k_3)B_\nu^{(4)}(k_4)M_{\mu\nu}(k_3,k_4,\cos\theta_{34})\ , \quad (4.17)$$

$$F_2(k_3,k_4,\cos\theta_{34})=\int g_2^{(3)}g_2^{(4)}k_3k_4(\cos\theta_{34}+\cos\theta_3\cos\theta_4)\frac{d\cos\theta_3d\cos\theta_4}{Q}=k_3k_4\sum_{\mu,\nu=0}^{1}C_\mu^{(3)}(k_3)C_\nu^{(4)}(k_4)[\cos\theta_{34}M_{\mu\nu}(k_3,k_4,\cos\theta_{34})+M_{\mu+1,\nu+1}(k_3,k_4,\cos\theta_{34})]\ , \quad (4.18)$$

where we have used $G_\rho^{(i)}=g_\rho^{(i)}/4\pi\lambda_iE_i^*$ [Eq. (4.3)]. The $g_\rho^{(i)}$ are given below in terms of the laboratory variables k_i and $\cos\theta_i$:

$$g_1^{(i)}=a_0^{(i)}+a_1^{(i)}E_i^*+a_2^{(i)}E_i^{*2}=A_0^{(i)}+A_1^{(i)}\cos\theta_i+A_2^{(i)}\cos^2\theta_i\ , \quad (4.19)$$

$$g_2^{(i)}=b_0^{(i)}+b_1^{(i)}E_i^*=C_0^{(i)}+C_1^{(i)}\cos\theta_i\ , \quad (4.20)$$

$$g_2^{(i)}k_i^*\cos\theta_i^*=(b_0^{(i)}+b_1^{(i)}E_i^*)(k_i^*\cos\theta_i^*)=B_0^{(i)}+B_1^{(i)}\cos\theta_i+B_2^{(i)}\cos^2\theta_i\ . \quad (4.21)$$

$$\begin{aligned}A_0^{(i)}&=a_0^{(i)}+a_1^{(i)}\gamma E_i+a_2^{(i)}\gamma^2E_i^2\ ,\\ B_0^{(i)}&=-\beta\gamma E_i(b_0^{(i)}+b_1^{(i)}\gamma E_i)\ ,\\ A_1^{(i)}&=-\beta\gamma k_i(a_1^{(i)}+2a_2^{(i)}\gamma E_i)\ ,\\ B_1^{(i)}&=\gamma k_i[b_0^{(i)}+b_1^{(i)}\gamma E_i(1+\beta^2)]\ ,\\ A_2^{(i)}&=\beta^2\gamma^2k_i^2a_2^{(i)},\quad B_2^{(i)}=-\beta\gamma^2k_i^2b_1^{(i)}\ ,\\ C_0^{(i)}&=b_0^{(i)}+b_1^{(i)}\gamma E_i,\quad C_1^{(i)}=-\beta\gamma k_ib_1^{(i)}\ .\end{aligned} \quad (4.22)$$

The integrals $M_{\mu\nu}$ are defined by

$$M_{\mu\nu}=\int d\cos\theta_4 d\cos\theta_3 \frac{\cos^\mu\theta_3\cos^\nu\theta_4}{Q} \quad (\mu,\nu=0,1,2)$$
$$=\int d\cos\theta_4\cos^\nu\theta_4 K_\mu(\theta_4) \tag{4.23}$$

with

$$K_\mu(\theta_4)=\int_{\Gamma_1(\theta_4)}^{\Gamma_2(\theta_4)}\frac{\cos^\mu\theta_3 d\cos\theta_3}{Q} .$$

The explicit, analytical expressions of K_μ and $M_{\mu\nu}$ are given in the Appendix.

2. Lepton-meson correlations

For lepton-meson correlations the integration of Eq. (4.14) has to be performed over the section of a straight line specified by the momenta k_3 and k_4 and the opening angle θ_{34} (see the Appendix, Fig. 20). The normalized distribution function $R=d^3\sigma/dk_3dk_4d\cos\theta_4$ can then be written as

$$R(k_3,k_4,\cos\theta_{34})=\frac{1}{4\pi\beta\gamma\lambda_3P_4^2}\frac{k_3^2k_4}{E_3E_4}\{F_0(k_3,k_4,\cos\theta_{34})+\xi_3\xi_4[F_1(k_3,k_4,\cos\theta_{34})u_1(\gamma)+F_2(k_3,k_4,\cos\theta_{34})u_2(\gamma)]\} . \tag{4.24}$$

Again the functions F_0, F_1, and F_2 can be factorized into momentum-dependent terms and into the integrals K_μ which depend on k_3, k_4, and $\cos\theta_{34}$:

$$F_0(k_3,k_4,\cos\theta_{34})=P_4\int g_1^{(3)}\frac{d\cos\theta_3}{Q}=P_4\sum_{\mu=0}^{2}A_\mu^{(3)}(k_3)K_\mu(\theta_4=\zeta_4) ,$$

$$F_1(k_3,k_4,\cos\theta_{34})=\frac{E_4-\gamma W_4}{\beta\gamma}\int g_2^{(3)}k_3^*\cos\theta_3^*\frac{d\cos\theta_3}{Q}=\frac{E_4-\gamma W_4}{\beta\gamma}\sum_{\mu=0}^{2}B_\mu^{(3)}(k_3)K_\mu(\theta_4=\zeta_4) ,$$

$$F_2(k_3,k_4,\cos\theta_{34})=k_3k_4\int g_2^{(3)}(\cos\theta_{34}+\cos\theta_3\cos\zeta_4)\frac{d\cos\theta_3}{Q}$$
$$=k_3k_4\sum_{\mu=0}^{1}C_\mu^{(3)}(k_3)[\cos\theta_{34}K_\mu(\theta_4=\zeta_4)+\cos\zeta_4K_{\mu+1}(\theta_4=\zeta_4)] .$$

[See Eqs. (4.19)–(4.22).]

For $\cos\zeta_3\le-\cos(\theta_{34}-\zeta_4)$ we obtain the definite integrals

$$K_0=\pi,\quad K_1=\pi\cos\zeta_4\cos\theta_{34} ,$$
$$K_2=\frac{\pi}{2}[(3\cos^2\theta_{34}-1)\cos^2\zeta_4+\sin^2\theta_{34}] . \tag{4.25}$$

For $-\cos(\theta_{34}-\zeta_4)\le\cos\zeta_3\le-\cos(\theta_{34}+\zeta_4)$ the integrals are

$$K_0=\frac{\pi}{2}-X(\zeta_4) ,$$
$$K_1=W(\zeta_4)-\cos\zeta_4\cos\theta_{34}\left[\frac{\pi}{2}-X(\zeta_4)\right] , \tag{4.26}$$
$$K_2=\tfrac{1}{2}(\cos\zeta_3-3\cos\zeta_4\cos\theta_{34})W(\zeta_4)$$
$$+\tfrac{1}{2}[(3\cos^2\theta_{34}-1)\cos^2\zeta_4+\sin^2\theta_{34}]\left[\frac{\pi}{2}-X(\zeta_4)\right] ,$$

where

$$X(\zeta_4)=\arcsin\frac{\cos\zeta_3+\cos\zeta_4\cos\theta_{34}}{\sin\zeta_4\sin\theta_{34}}$$

and

$$W(\zeta_4)=\sqrt{\sin^2\zeta_3\sin^2\zeta_4-(\cos\theta_{34}+\cos\zeta_3\cos\zeta_4)^2} .$$

E. Momentum-momentum distributions

1. General considerations

The general normalized distribution $S(k_3,k_4)=d^2\sigma/dk_3dk_4$ can be obtained by integrating $R(k_3,k_4,\cos\theta_{34})$ [Eq. (4.14)]:

$$\frac{d^2\sigma}{dk_3dk_4}=\int_{-\cos(\theta_3-\theta_4)}^{-\cos(\theta_3+\theta_4)}\frac{d^3\sigma}{dk_3dk_4d\cos\theta_{34}}d\cos\theta_{34} ,$$

$$S(k_3,k_4)=4\pi^2\frac{k_3^2k_4^2}{E_3E_4}\int d\cos\theta_3 d\cos\theta_4E_3^*E_4^*[G_1^{(3)}G_1^{(4)}+\xi_3\xi_4G_2^{(3)}G_2^{(4)}(k_3^*\cos\theta_3^*)(k_4^*\cos\theta_4^*)u_1(\gamma)] . \tag{4.27}$$

Note that the last term in Eq. (4.14) has vanished due to the integration. This term plays an important role for the distribution $R(\theta_3,\theta_4,\cos\theta_{34})$ at low energies by enhancing the sensitivity to the ξ parameter, while it can be neglected at higher energies due to the factor $u_2(\gamma)=1/(2\gamma^2+1)$.

2. *Normalized distributions in the laboratory system*

The distributions $S(k_3,k_4)$ are considerably simpler than $R(k_3,k_4,\cos\theta_{34})$ due to the fact that the integration over $\cos\theta_3$ is independent of $\cos\theta_4$. Thus for leptons

$$\cos\zeta_i \le \cos\theta_i \le 1$$

and for mesons

$$\cos\theta_i = \cos\zeta_i \ .$$

The normalized distribution function for any combination of leptons and mesons can therefore be written as

$$S(k_3,k_4)=[H_0^{(3)}(k_3)H_0^{(4)}(k_4) + \xi_3\xi_4 H_1^{(3)}(k_3)H_1^{(4)}(k_4)u_1(\gamma)] \ , \quad (4.28)$$

where

$$H_0^{(i)}(k_i)=\frac{1}{2\lambda_i}\frac{k_i^2}{E_i}\int_{\cos\zeta_i}^{1} g_1^{(i)} d\cos\theta_i = \frac{1}{2\lambda_i}\frac{k_i^2}{E_i}\sum_{\mu=0}^{2}\frac{1}{\mu+1}A_\mu^{(i)}(k_i)(1-\cos^{\mu+1}\zeta_i) \quad (4.29)$$

and

$$H_1^{(i)}(k_i)=\frac{1}{2\lambda_i}\frac{k_i^2}{E_i}\int_{\cos\zeta_i}^{1} g_2^{(i)}(k_i^*\cos\theta_i^*) d\cos\theta_i = \frac{1}{2\lambda_i}\frac{k_i^2}{E_i}\sum_{\mu=0}^{2}\frac{1}{\mu+1}B_\mu^{(i)}(k_i)(1-\cos^{\mu+1}\zeta_i) \quad (4.30)$$

for leptons, and

$$H_0^{(i)}(k_i)=\frac{1}{2\beta\gamma P_4}\frac{k_i}{E_i} \quad (4.31)$$

and

$$H_1^{(i)}(k_i)=\frac{1}{2\beta\gamma P_4^2}\frac{E_4-\gamma W_4}{\beta\gamma} \quad (4.32)$$

for mesons.

F. Momentum distributions

Single lepton spectra from unpolarized τ's have been analyzed up to now only in terms of the Michel parameter ρ. These spectra, however, depend also on the low-energy parameter η (see Secs. III B 2 and IV C 2), which is strongly correlated with ρ. Therefore ρ and η should be evaluated simultaneously, both for the decay into an electron and into a muon. The normalized decay probability in terms of the laboratory variables is given by $H_0^{(i)}(k_i)$ in Eq. (4.29).

V. MUON POLARIZATION

A. General considerations

In muon decay, the polarization of positrons from stopped muons is measured. Because of the short lifetime (≈ 100 fs) of the τ lepton, this method is not feasible for leptonic τ decay. As noted in Sec. III C one can stop the positive muon from τ^+ decay and use their decay asymmetry as an excellent analyzer. Because of the large momentum band of the emitted muons it is only possible to stop muons in a certain momentum region. In contrast with the correlation experiments discussed in the previous section, the knowledge of the τ^- decay is necessary only as far as to identify the μ^+ as the decay product of the τ^+ by the identification of the decay products of the τ^-.

B. Polarization and figure of merit

We have transformed the most general decay spectrum as given by Scheck[5] from the c.m. system of the τ^+ with velocity β into the laboratory system, thereby integrating over the azimuthal angle. The resulting distribution $d^2\Gamma/dk_\mu d\cos\theta_\mu$ was also integrated over the unobservable laboratory angle θ_μ. The longitudinal polarization ζ_μ of the μ^+ of momentum k_μ is given by

$$\zeta_\mu=\frac{\sigma_+-\sigma_-}{\sigma_++\sigma_-} \ , \quad (5.1)$$

where σ_+ and σ_- are the decay rates for emission of a muon with spin parallel, respectively, antiparallel to its line of flight in the laboratory system based on n_0 events. The figure of merit of a polarization measurement is defined as $\zeta_\mu^2\sigma$ with $\sigma=\frac{1}{2}(\sigma_++\sigma_-)$. We use the notation of Sec. IV for the kinematics of leptonic τ decays except for the maximum angle of emission ζ_μ of the muon which is called Θ_μ in this section to avoid confusion with the μ polarization. The polarization and the figure of merit can then be written as

$$\zeta_\mu=\frac{H_2}{F_1+F_3} \quad (5.2)$$

and

$$\frac{d\zeta_\mu^2\sigma}{dk_\mu}=n_0\frac{H_2^2}{F_1+F_3}\Big/\int(F_1+F_3)dk_\mu \quad (5.3)$$

with

$$F_i=\frac{k_\mu^2}{2\lambda_\mu E_\mu}\sum_{\nu=0}^{2} f_{i\nu}\frac{1-\cos^{\nu+1}\Theta_\mu}{\nu+1}$$

and

$$H_2=\frac{k_\mu^2}{2\lambda_\mu E_\mu}\sum_{\nu=0}^{2}h_{2\nu}\frac{1-\cos^{\nu+1}\Theta_\mu}{\nu+1}\ ,$$

$$f_{11}=2a_1\gamma E_\mu(W_\mu-\gamma E_\mu)+a_4[P_\mu^2-(W_\mu-\gamma E_\mu)^2]\ ,$$

$$f_{12}=2\beta\gamma k_\mu[\alpha_1(2\gamma E_\mu-W_\mu)-a_4(W_\mu-\gamma E_\mu)]\ ,$$

$$f_{13}=-\beta^2\gamma^2k_\mu^2(2a_1+a_4)\ ,$$

$$f_{31}=2m_\mu a_9(W_\mu-\gamma E_\mu)\ ,$$

$$f_{32}=2m_\mu a_9\beta\gamma k_\mu,\quad f_{33}=0\ ,$$

$$h_{21}=\gamma k_\mu\{2a_6(W_\mu-\gamma E_\mu)+a_8[P_\mu+(W_\mu-\gamma E_\mu)]\}\ ,$$

$$h_{22}=\beta(2a_6[\gamma^2k_\mu^2-\gamma E_\mu(W-\gamma E_\mu)]+a_8\{\gamma^2k_\mu^2-\gamma E_\mu[P_\mu+(W_\mu-\gamma E_\mu)]\})\ ,$$

$$h_{23}=-\beta^2\gamma^2k_\mu E_\mu(2a_6+a_8)\ ,$$

The a_j are functions of the decay parameters:

$$a_1=6(9-10\rho_\mu),\quad a_4=24\rho_\mu\ ,$$

$$a_6=-15\xi_\mu+20\xi_\mu\delta_\mu-9\xi'_\mu\ ,$$

$$a_8=6\xi_\mu-8\xi_\mu\delta_\mu-18\xi'_\mu,\quad a_9=54\eta_\mu\ .$$

We note that if ξ_μ and δ_μ are close to their $V-A$ values of $+1$ and $+\frac{3}{4}$, respectively, $a_6\approx-9\xi'_\mu$ and $a_8\approx-18\xi'_\mu$, so that the term H_2 in the numerator of Eq. (5.2) is directly proportional to ξ'_μ.

VI. RESULTS

A. General considerations

The analytical expressions derived in Sec. IV and in the Appendix for the distribution functions $R(k_3,k_4,\cos\theta_{34})$ and $S(k_3,k_4)$ allows us to use the method of maximum likelihood to estimate the covariance matrix V_{nm}, where n and m designate any two of the decay parameters $x_n,x_m=\rho$, η, δ, or ξ. The matrix element of the inverse matrix V^{-1} is given by

$$V_{nm}^{-1}=\sum_{\rm PS}\sigma A_nA_m\ , \tag{6.1}$$

where $\sigma=n_0R$ or n_0S, and n_0 is the total number of events for the given final state. The sensitivity A_n is

$$A_n=\frac{1}{\sigma}\frac{\partial\sigma}{\partial x_n}\ , \tag{6.2}$$

and $\sum_{\rm PS}$ denotes numerical integration over phase space. We further introduce the figure of merit (or information) M_n:

$$M_n=\sigma A_n^2\ .$$

Note that

$$\sum_{\rm PS}M_n=(V^{-1})_{nn} \tag{6.3}$$

and, for uncorrelated parameters x_i,

$$\sigma_n=\frac{1}{\left[\sum_{\rm PS}M_n\right]^{1/2}}\ , \tag{6.4}$$

where σ_n is the statistical error of the parameter x_n. In Secs. VI B–VI D we discuss the angular and energy dependence of the figures of merit of the different decay parameters, based on $n_0=10^7$ events for each given final state. The use of the figure of merit instead of the statistical error has the advantage that contributions of different parts of phase space are additive to the total figure of merit. Although due to error correlations the true statistical errors will be larger than $1/(\sum M_n)^{1/2}$ (for ρ and η by 20–50 %, for δ and ξ by 50–100 %), we prefer not to include the error correlations in the discussion of the angular and energy dependence of the figure of merit; we list, however, the values of the error correlations at one energy and note that they depend only weakly on energy.

In Sec. VI E, finally, we calculate the error matrix and error correlations for all of the ten decay parameters ρ_μ, η_μ, δ_μ, ξ_μ, ρ_e, η_e, δ_e, ξ_e, ξ_π, and ξ_K (Ref. 32) on the basis of 10^7 produced $\tau^+\tau^-$ pairs and using the measured branching ratios. For all of the calculations in Sec. VI the decay parameters have been given the values as predicted by $V-A$, i.e., $\rho_\mu=\rho_e=\frac{3}{4}$, $\eta_\mu=\eta_e=0$, $\delta_\mu=\delta_e=\frac{3}{4}$, $\xi_\mu=\xi_e=1$, and $\xi_\pi=\xi_K=-1$.

B. Contour diagrams

The contour diagrams of the sensitivity A_n and of the figures of merit (FM or M_n) for the distributions $R(k_3,k_4,\cos\theta_{34})$ are characterized by the strongly varying shapes of the kinematically allowed region in (k_3,k_4)-space as a function of the opening angle θ_{34}, and by a rich pattern of positive and negative values of A_n. The distributions of the FM's are especially valuable for designing an experiment since they show directly the effect of momentum cuts on the precision of the measurements. Figure 3 shows the contour lines (in percent) for both A_δ and M_δ at $E_0=10.55$ GeV and $\cos\theta_{34}=-0.99$, the contour lines for the same angle and energy for A_ξ and M_ξ are shown in Fig. 4, where we have chosen μ^+e^- in the final state.

Although it would be very important for a detailed analysis especially of the asymmetry parameters δ and ξ to keep the $\cos\theta_{34}$ dependence, as will be shown below, the following diagrams are evaluated for the rate $S(k_3,k_4)$ only in order to limit their number to the absolutely necessary. All the figures but the last, we compare the results found for μ^+e^- in the final state with those found for $\mu^+\pi^-$. Figure 5 shows the rate distributions. It is maximal for low lepton and high meson energy. Figure 6 shows M_{ρ_μ} which is largest at *high* muon momenta with a second maximum at lower momenta. Note that this (partial) FM is a differential quantity, it is therefore the *area* between neighboring lines that counts. Clearly the measurement of ρ_μ is easy to achieve with muon momenta between 3 and 5 GeV/c and electron momenta below 2 GeV/c or pion momenta above 3 GeV/c.

The determination of η_μ is somewhat more difficult, as

can be seen in Fig. 7, since the main contribution stems from muon momenta below 1 GeV/c where muons are difficult to identify. It will be shown below, however, that the total FM is large enough that even a lower muon threshold of 1 GeV/c still allows a precise measurement of η_μ.

The distributions for δ_μ in Fig. 8 show that δ_μ can be determined best at high particle momenta, independent of the type of particle. This is also true for the determination of the ξ parameter (see Fig. 9) which has two additional strong maxima where one of the leptons is low in energy.

The last diagram in this series, Fig. 10, finally shows the distributions of the rate and of M_{ξ_π} for $\pi^+\pi^-$ in the final state. M_{ξ_π} is maximal where the rate is vanishing, since this results in a high sensitivity for ξ_π.

C. Angular distributions of the figures of merit

The figures of merit for $R(k_3,k_4,\cos\theta_{34})$ were integrated numerically over the momenta of the two detected particles. Figures 11 and 12 show the resulting angular distributions for the four decay parameters for μ^+e^- and $\mu^+\pi^-$, respectively, and at 4-GeV total energy, while Figs. 13 and 14 display the same distributions at 10.55 GeV, slightly below the Υ_{4S} resonance.

The distributions for ρ_μ and η_μ are decreasing monotonously with increasing $\cos\theta_{34}$, where the total decrease is small at 4 GeV and large at 10.55 GeV due to the Lorentz boost. The distributions for δ and ξ behave quite differently. They exhibit an energy dependent minimum with a subsequent rise. Again the total FM is equal to the integral which has been indicated by shading the area below the curves. What comes as a surprise is that even at the higher energy, the strongest contribution to the total integral stems from angles $\theta_{34}<155°$ which is important if one has to make cuts on collinear background events.

D. Energy dependence of the figures of merit

The angular distributions of the FM's (see Sec. IV D) were numerically integrated over $\cos\theta_{34}$ resulting in a total FM as a function of the total energy E_0. These energy

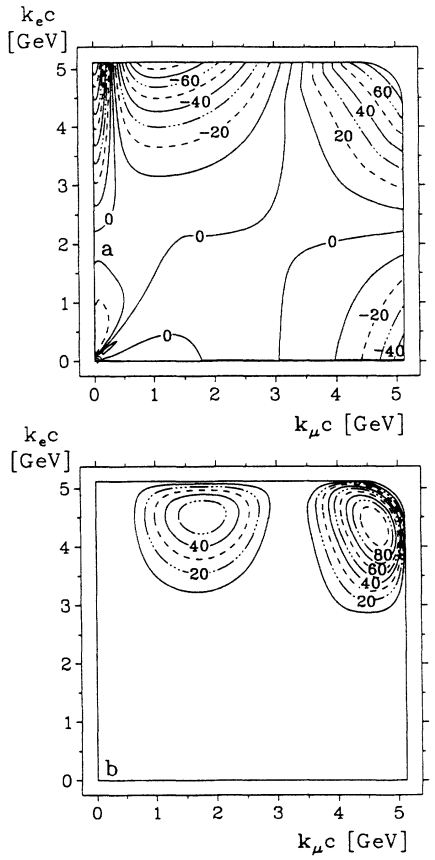

FIG. 3. Contour lines (in percent) of the sensitivity (a) and the figure of merit (b) for the leptonic decay parameter δ_μ as determined from the correlated distribution $R(k_\mu,k_e,\cos\theta_{\mu e}=-0.99)$ for the reactions $e^+e^-\to\tau^+\tau^-\to(\mu^+\nu_\mu\bar{\nu}_\tau)(e^-\bar{\nu}_e\nu_\tau)$ at 10.55-GeV total energy.

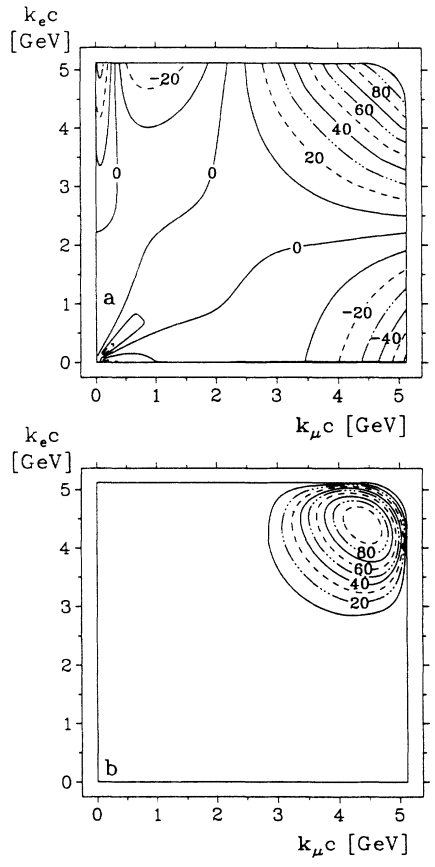

FIG. 4. Contour lines (in percent) of the sensitivity (a) and the figure of merit (b) for the leptonic decay parameter ξ_μ as determined from the correlated distribution $R(k_\mu,k_e,\cos\theta_{\mu e}=-0.99)$ for the reactions $e^+e^-\to\tau^+\tau^-\to(\mu^+\nu_\mu\bar{\nu}_\tau)(e^-\bar{\nu}_e\nu_\tau)$ at 10.55-GeV total energy.

distributions are compared in Figs. 15 and 16 with the distributions obtained by integrating the FM's of $S(k_3,k_4)$ over the particle momenta. Here again the scalar spectrum shape parameters ρ_μ and η_μ show a similar behavior. At $\tau^+\tau^-$ production threshold the particle momenta and emission angles are independent from each other. Therefore the full information about ρ_μ and η_μ can be obtained by measuring k_3 and k_4 alone already. With increasing total energy the laboratory momenta depend on both c.m. momentum and angle due to the Lorentz transformation. Therefore the FM's of δ and η, measured via $S(k_3,k_4)$ decrease with energy until they reach a plateau at about 9 GeV. Measuring $R(k_3,k_4,\cos\theta_{34})$ saves some of the angular information and therefore leads to a higher plateau.

The distributions for δ and ξ, however, which describe the anisotropic part of the spectrum, vanish at threshold if θ_{34} is not measured and retain a finite value in the opposite case. Here the decreasing effect described in the case of δ and η is more than compensated by the spin correlation which strongly increases with energy [characterized by the factor $u_1(\gamma)$ in Eq. (4.14), for example]. Especially for the final state μ^+e^- the quality of the measurement is vastly increased by including the θ_{34} dependence. For the final state $\mu^+\pi^-$ the effect is also seen, but much less pronounced. The reason is that for mesons the information on the c.m. decay angle θ^* is already contained uniquely in the momentum, while for leptons the momentum alone is not sufficient to determine the c.m. decay angle, since one also needs to know the laboratory angle. While this observable is experimentally not accessible, the opening angle θ_{34} contains at least partially this information.

Finally, for completeness, Fig. 17 shows the distribution of ξ_π for $\pi^+\pi^-$ in the final state with a corresponding behavior.

E. Tables for the spectrum parameters ρ, η, ξ, and δ

In the discussion so far only the final states μ^+e^-, $\mu^+\pi^-$, and $\pi^+\pi^-$ were treated. For energies not directly at threshold, the muon can be easily substituted by the electron and the pion by the kaon with virtually the same results.

We emphasize, however that we regard the decay parameters describing τ decay into a muon as completely independent from those describing τ decay into an elec-

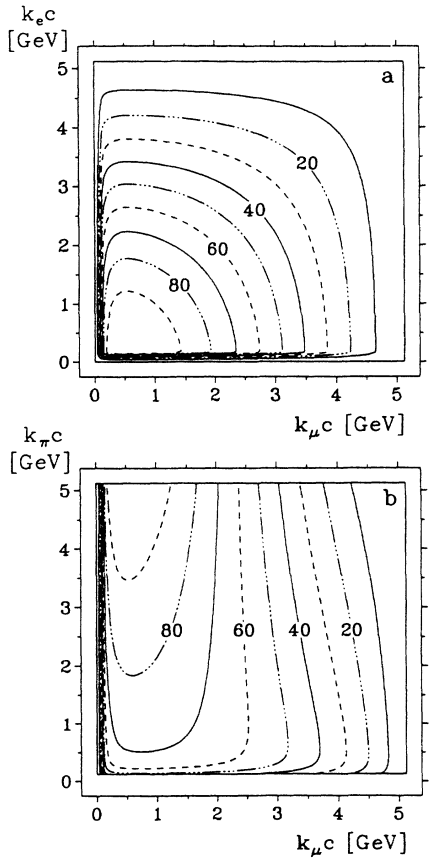

FIG. 5. Contour lines (in percent) of the rates $S(k_\mu,k_e)$ (a) and $S(k_\mu,k_\pi)$ (b) for the reactions $e^+e^-\to\tau^+\tau^-\to(\mu^+\nu_\mu\bar{\nu}_\tau)(e^-\bar{\nu}_e\nu_\tau)$ and $e^+e^-\to\tau^+\tau^-\to(\mu^+\nu_\mu\bar{\nu}_\tau)$ at 10.55-GeV total energy.

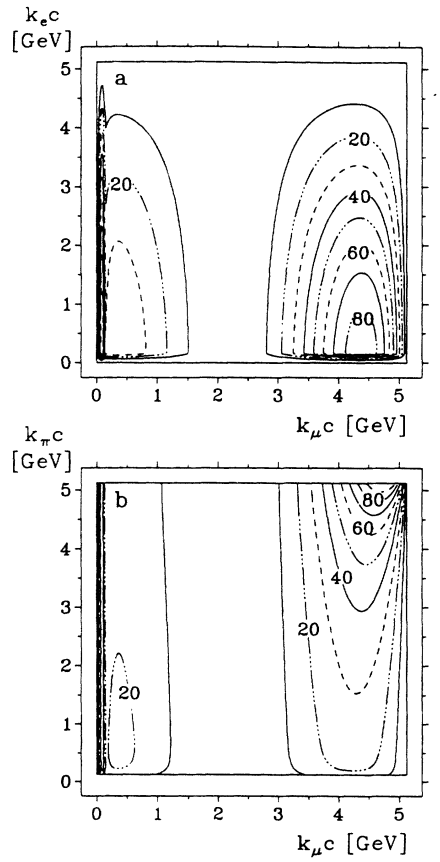

FIG. 6. Contour lines (in percent) of the figure of merit for the leptonic decay parameter ρ_μ as determined from the correlated distributions $S(k_\mu,k_e)$ for the reaction $e^+e^-\to\tau^+\tau^-\to(\mu^+\nu_\mu\bar{\nu}_\tau)(e^-\bar{\nu}_e\nu_\tau)$ (a) and $e^+e^-\to\tau^+\tau^-\to(\mu^+\nu_\mu\bar{\nu}_\tau)(\pi^-\nu_\tau)$ (b) at 10.55-GeV total energy.

TABLE I. Figures of Merit for the leptonic τ decay parameters. For each of the final states 10^7 events are assumed, independent of its particular branching ratio.

	$S(k_3,k_4)$: final state			$R(k_3,k_4,\theta_{34})$: final state		
	$\mu\mu$	μe	$\mu\pi$	$\mu\mu$	μe	$\mu\pi$
			$E_0=4$			
ρ_μ	4 639 000	2 336 000	2 343 000	5 508 000	2 660 000	3 037 000
η_μ	2 594 000	804 100	802 000	2 642 000	827 700	854 100
η_e		28			29	
δ_μ	22 780	6 580	46 740	72 880	22 660	121 300
ξ_μ	17 590	4 360	31 280	62 180	15 450	78 520
			$E_0=10.55$ GeV			
ρ_μ	1 816 000	945 500	1 012 000	4 247 000	1 841 000	2 416 000
η_μ	2 129 000	573 700	575 800	2 412 000	700 800	752 800
η_e		17			24	
δ_μ	55 000	19 180	164 100	164 100	49 800	266 000
ξ_μ	76 560	19 040	154 800	146 370	36 300	186 200

tron. We can see no convincing reason to do otherwise, and therefore we have labeled the decay constants correspondingly. The same arguments apply for semileptonic decays, where ξ_π is treated as being independent of ξ_K. Equalizing corresponding decay constants can increase the figure of merit, depending on the correlation coefficient, up to a factor of 4 (in the case of $\xi_\mu=\xi_e$, for example). In Table I we have summarized our results for

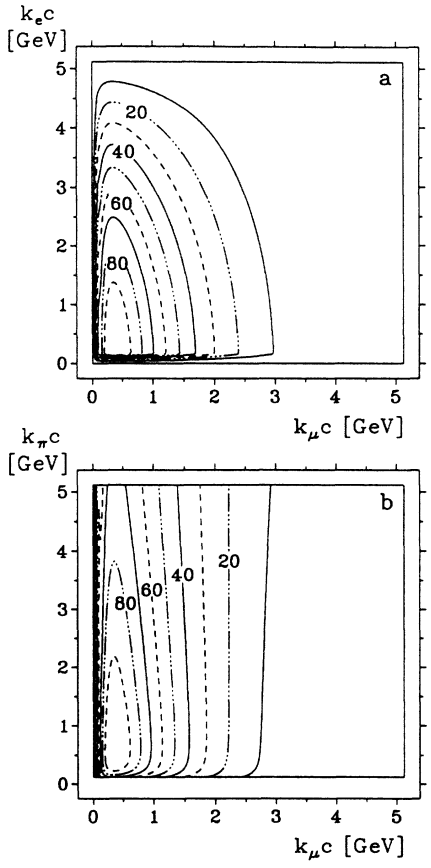

FIG. 7. Contour lines (in percent) of the figure of merit for the leptonic decay parameter η_μ as determined from the correlated distributions $S(k_\mu,k_e)$ for the reaction $e^+e^-\to\tau^+\tau^-\to(\mu^+\nu_\mu\bar{\nu}_\tau)(e^-\bar{\nu}_e\nu_\tau)$ (a) and $e^+e^-\to\tau^+\tau^-\to(\mu^+\nu_\mu\bar{\nu}_\tau)(\pi^-\nu_\tau)$ (b) at 10.55-GeV total energy.

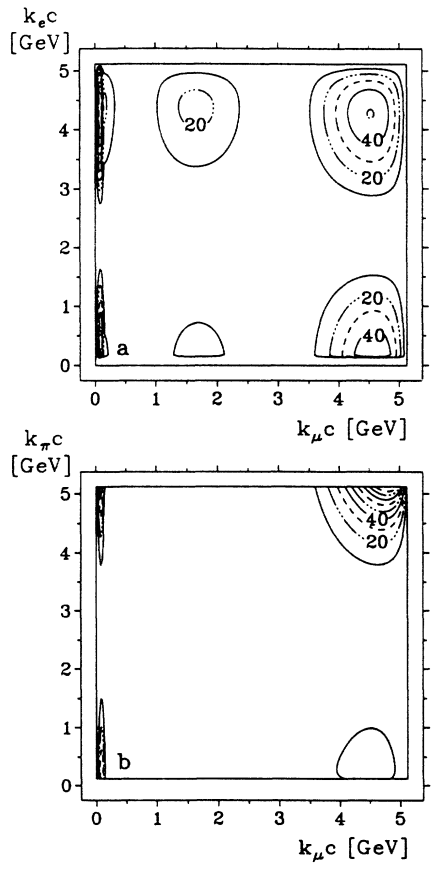

FIG. 8. Contour lines (in percent) of the figure of merit for the leptonic decay parameter δ_μ as determined from the correlated distributions $S(k_\mu,k_e)$ for the reaction $e^+e^-\to\tau^+\tau^-\to(\mu^+\nu_\mu\bar{\nu}_\tau)(e^-\bar{\nu}_e\nu_\tau)$ (a) and $e^+e^-\to\tau^+\tau^-\to(\mu^+\nu_\mu\bar{\nu}_\tau)(\pi^-\nu_\tau)$ (b) at 10.55-GeV total energy.

$E_0=4$ GeV and $E_0=10.55$ GeV. For the reasons mentioned above we present the FM's not for all possible final states, but restrict ourselves to μ^+e^- (two different leptons), $\mu^+\mu^-$ (two identical leptons) and to $\mu^+\pi^-$ (lepton and meson).

Finally we derive best possible errors for the decay parameters. Here we assume 10^7 produced $\tau^+\tau^-$ pairs and make use of the measured branching ratios η_i (Ref. 33) into μ, e, π, and K. For each final state the error matrix was calculated. Tables II and III show the errors for the decay parameters. We note that the parameters ξ_3 and ξ_4 in the decay distribution (4.14) appear only as the product $\xi_3\xi_4$. Therefore for the final states $\mu^+\mu^-$, e^+e^-, $\pi^+\pi^-$, and K^+K^-, $|\xi|$ can be determined. For final states with two different particles, ξ_3 and ξ_4 are 100% correlated. These values are also given with the assumption that $\xi_4\equiv 1$ and are marked by an asterisk.

The 100% correlation between ξ_3 and ξ_4 can, however, be removed by the joint analysis of all possible combinations between the four particles μ, e, π, and K. This results in a 10×10 error matrix for their decay parameters, and it reduces the correlations between most of the parameters. Table IV shows the correlation matrix for the distribution $R(k_3,k_4,\cos\theta_{34})$ at a total energy $E_0=10.55$ GeV. The correlation matrices for the distribution $S(k_3,k_4)$ and at lower energies are similar and therefore

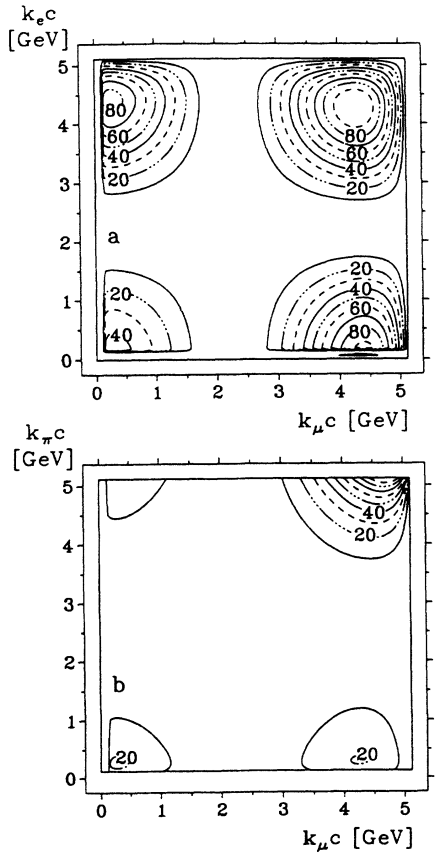

FIG. 9. Contour lines (in percent) of the figure of merit for the leptonic decay parameter ξ_μ as determined from the correlated distributions $S(k_\mu,k_e)$ for the reaction $e^+e^-\to\tau^+\tau^-\to(\mu^+\nu_\mu\bar{\nu}_\tau)(e^-\bar{\nu}_e\nu_\tau)$ (a) and $e^+e^-\to\tau^+\tau^-\to(\mu^+\nu_\mu\bar{\nu}_\tau)(\pi^-\nu_\tau)$ (b) at 10.55-GeV total energy.

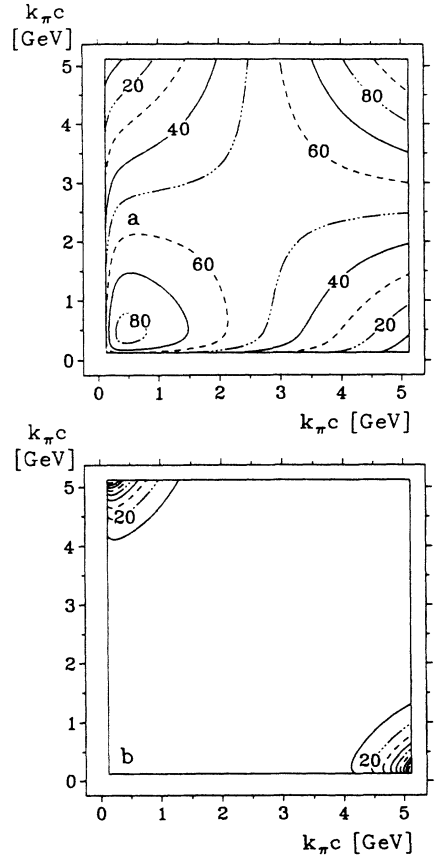

FIG. 10. Contour lines (in percent) of the rate $S(k_\pi,k_\pi)$ (a) and the figure of merit for the decay parameter ξ_π (b) for the reaction $e^+e^-\to\tau^+\tau^-\to(\pi^+\bar{\nu}_\tau)(\pi^-\nu_\tau)$ at 10.55-GeV total energy.

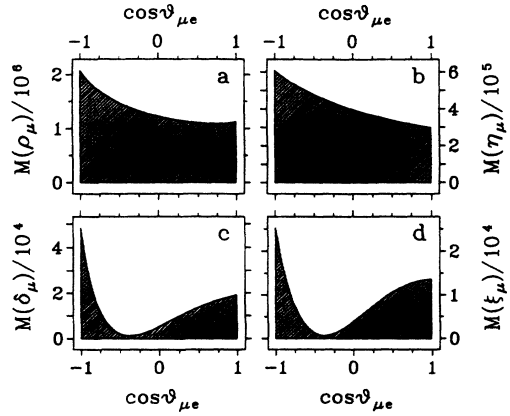

FIG. 11. Angular distributions of the figures of merit for the leptonic decay parameters ρ_μ, η_μ, δ_μ, and ξ_μ as determined from the correlated distribution $R(k_\mu,k_e,\cos\theta_{\mu e})$ for the reactions $e^+e^-\to\tau^+\tau^-\to(\mu^+\nu_\mu\bar{\nu}_\tau)(e^-\bar{\nu}_e\nu_\tau)$ at 4-GeV total energy.

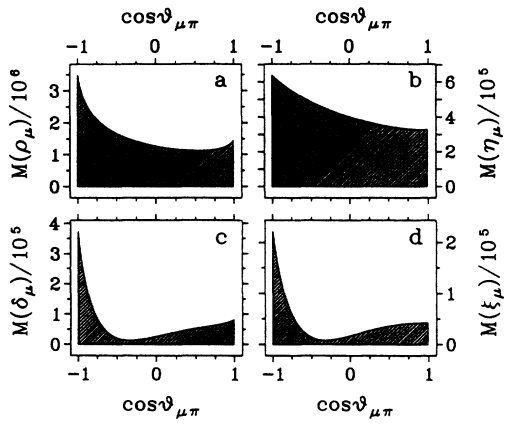

FIG. 12. Angular distributions of the figures of merit for the leptonic decay parameters ρ_μ, η_μ, δ_μ, and ξ_μ as determined from the correlated distribution $R(k_\mu,k_\pi,\cos\theta_{\mu\pi})$ for the reactions $e^+e^-\to\tau^+\tau^-\to(\mu^+\nu_\mu\bar{\nu}_\tau)(\pi^-\nu_\tau)$ at 4-GeV total energy.

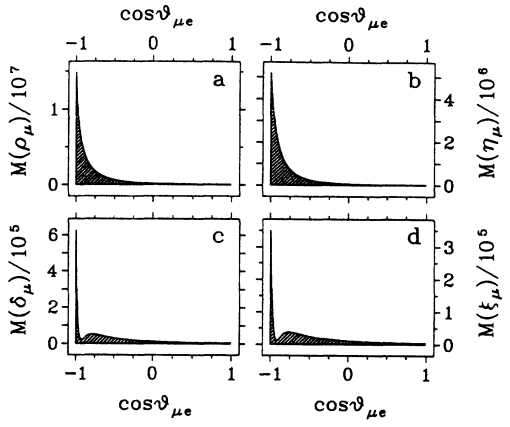

FIG. 13. Angular distributions of the figures of merit for the leptonic decay parameters ρ_μ, η_μ, δ_μ, and ξ_μ as determined from the correlated distribution $R(k_\mu,k_e,\cos\theta_{\mu e})$ for the reactions $e^+e^-\to\tau^+\tau^-\to(\mu^+\nu_\mu\bar{\nu}_\tau)(e^-\bar{\nu}_e\nu_\tau)$ at 10.55-GeV total energy.

have been omitted. As one sees the main correlations left are those between the Michel parameter ρ and the low-energy parameter η for the same kind of lepton, both of which describe the isotropic part of the spectrum in the c.m. system, and between δ and ξ for the same kind of lepton which together describe the anisotropic part of the spectrum in the c.m. system.

In Table V the statistical errors are given for the ten

TABLE II. Statistical errors (in units of 10^{-3}) for the leptonic decay parameters and the two semi-leptonic decay parameters ξ_π and ξ_K which can be achieved with an ideal detector by measuring the various correlated momentum distributions $S(k_3,k_4)$ and based on 10^7 produced $\tau^+\tau^-$ pairs. The measured branching ratios (Ref. 33) are taken into account. Quantities designated by an asterisk are only measured in the combination $\xi_3\xi_4$ and are therefore 100% correlated.

Total energy E_0 (GeV)	Decay parameter		Particles detected μ	e	π	K
4.0	ρ_μ	μ	2.9	3.7	4.0	16.2
	η_μ		3.9	8.3	6.9	27.7
	δ_μ		92.4	93.2	45.7	184.8
	ξ_μ		105.2	149.7*	55.9*	226.1*
	ρ_e	e	3.6	2.9	4.0	16.0
	η_e		1380.6	703.2	1148.8	4647.3
	δ_e		92.3	93.1	45.6	184.4
	ξ_e		149.7*	106.6	56.2*	227.2*
	ξ_π	π	55.9*	56.2*	9.9	56.9*
	ξ_K	K	226.1*	227.2*	56.9*	162.6
10.55	ρ_μ	μ	4.4	6.4	5.6	22.6
	η_μ		4.0	17.9	7.2	29.2
	δ_μ		39.5	39.1	19.0	76.7
	ξ_μ		33.5	47.3*	19.5*	78.8*
	ρ_e	e	6.9	4.4	5.6	22.7
	η_e		3363.4	772.3	1364.0	5518.3
	δ_e		36.7	37.4	17.9	72.5
	ξ_e		47.3*	33.3	19.3*	77.9*
	ξ_π	π	19.5*	19.3*	4.0	23.0*
	ξ_K	K	78.8*	77.9*	23.0*	65.8

TABLE III. Statistical errors (in units of 10^{-3}) for the leptonic decay parameters and the two semileptonic decay parameters ξ_π and ξ_K which can be achieved with an ideal detector by measuring the various correlated momentum-angular distributions $R(K_3,k_4,\cos\theta_{34})$ and based on 10^7 produced $\tau^+\tau^-$ pairs. The measured branching ratios (Ref. 33) are taken into account. Quantities designated by an asterisk are only measured in the combination $\xi_3\xi_4$ and are therefore 100% correlated.

Total energy E_0 (GeV)	Decay parameter		Particles detected μ	e	π	K
4.0	ρ_μ	μ	2.9	3.6	3.6	14.4
	η_μ		3.9	8.0	6.7	27.1
	δ_μ		38.6	40.9	21.4	87.7
	ξ_μ		43.2	60.7*	26.6*	109.4*
	ρ_e	e	3.5	2.9	3.5	14.1
	η_e		1324.7	697.5	1107.9	4485.2
	δ_e		38.5	37.1	20.4	83.5
	ξ_e		60.7*	42.7*	26.2*	107.8*
	ξ_π	π	26.6*	26.2*	9.9	56.9*
	ξ_K	K	109.4*	107.8*	56.9*	162.6
10.55	ρ_μ	μ	3.1	4.4	3.8	15.4
	η_μ		3.9	9.8	6.9	27.9
	δ_μ		26.9	28.5	14.6	58.5
	ξ_μ		29.0	40.9*	17.5*	70.8*
	ρ_e	e	4.3	3.1	3.8	15.3
	η_e		1674.8	724.0	1197.3	4751.2
	δ_e		27.0	26.2	14.0	56.0
	ξ_e		40.9*	28.8	17.3*	70.0*
	ξ_π	π	17.5*	17.3*	4.0	23.0*
	ξ_K	K	70.8*	70.0*	23.0*	65.8

different coupling constants. Errors have also been derived for the probabilities $P_R^\tau(\mu)$ and $P_R^\tau(e)$ of the τ in the two leptonic decays to be right handed (see also Sec. II B):

$$P_R^\tau(l)=\tfrac{1}{2}[1+\tfrac{1}{9}(3\xi_l-16\xi_l\delta_l)]\ , \tag{6.5}$$

where $l=e,\mu$. The statistical error of $P_R^\tau(l)$ is given by

$$\Delta P_R^\tau(l)=[(\tfrac{1}{2}\sigma_\xi)^2+2\rho_{\delta\xi}(\tfrac{1}{2}\sigma_\xi)(\tfrac{8}{9}\sigma_\delta)+(\tfrac{8}{9}\sigma_\delta)^2]^{1/2}\ , \tag{6.6}$$

where again $\delta=\frac{3}{4}$ and $\xi=1$ have been assumed. $\rho_{\delta\xi}$ is the correlation between δ and ξ. $P_R^\tau(l)$ is the most important parameter to be determined in the measurement of the decay spectra, as can be seen from Eq. (2.9):

TABLE IV. Error correlation (in %) between the τ decay parameters at a total energy $E_0=10.55$ GeV. The correlations have been obtained from a joint analysis of all possible combinations of μ, e, π, and K for the momenta-angular distribution $R(k_3,k_4,\cos\theta_{34})$. Correlations with absolute value smaller than 5% have been suppressed for better readability.

	ρ_μ	η_μ	δ_μ	ξ_μ	ρ_e	η_e	δ_e	ξ_e	ξ_π	ξ_K
ρ_μ	100	46		11	−8	−12				
η_μ	46	100		5	−12	−24				
δ_μ			100	−76						
ξ_μ	11	5	−76	100					−12	
ρ_e	−8	−12			100	46		12		
η_e	−12	−24			46	100		5		
δ_e							100	−74		
ξ_e					12	5	−74	100	−12	0
ξ_π				−12				−12	100	−10
ξ_K									−10	100

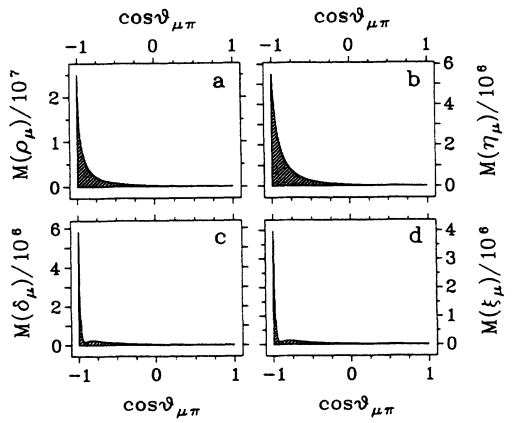

FIG. 14. Angular distributions of the figures of merit for the leptonic decay parameters ρ_μ, η_μ, δ_μ, and ξ_μ as determined from the correlated distribution $R(k_\mu,k_\pi,\cos\theta_{\mu\pi})$ for the reactions $e^+e^-\to\tau^+\tau^-\to(\mu^+\nu_\mu\bar{\nu}_\tau)(\pi^-\nu_\tau)$ at 10.55-GeV total energy.

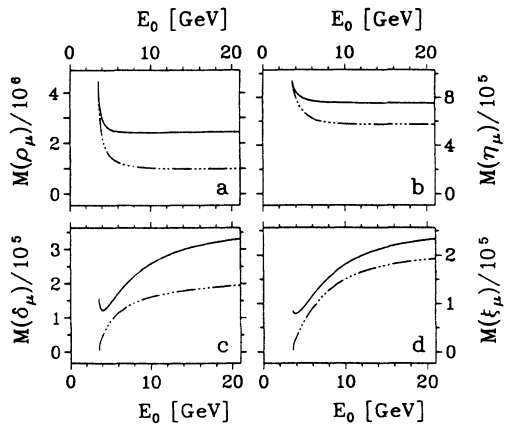

FIG. 16. Total figures of merit for the leptonic decay parameters ρ_μ, η_μ, δ_μ, and ξ_μ as a function of the total beam energy E_0. The curves are derived from the correlated distribution $R(k_\mu,k_\pi,\cos\theta_{\mu\pi})$ for the reactions $e^+e^-\to\tau^+\tau^-\to(\mu^+\nu_\mu\bar{\nu}_\tau)(\pi^-\nu_\tau)$ by numerical integration.

$$P_R^\tau(l)=\tfrac{1}{4}|g_{RR}^S|^2+\tfrac{1}{4}|g_{LR}^S|^2+|g_{RR}^V|^2+|g_{LR}^V|^2+3|g_{LR}^T|^2 .$$

It measures the contributions of all of the five interactions with right-handed τ leptons. Thus a small $P_R^\tau(l)$ gives simultaneously stringent limits to five of the ten complex coupling constants describing leptonic τ decay.

We find that due to the large negative correlation $\rho_{\delta\xi}$, $P_R^\tau(l)$ can be measured more precisely than both δ_l and ξ_l. At 10.55 GeV total energy and measuring $R(k_3,k_4,\cos\theta_{34})$ for all combinations of μ, e, π, and K for $10^7\tau^+\tau^-$ pairs produced we find $\Delta P_R^\tau(l)\approx 6.6\times10^{-3}$. This results in a limit, for example, for the $V+A$ coupling constant $|g_{RR}^V|<0.081$ which is comparable with the corresponding upper limit obtained in μ decay.[1]

The Michel parameters ρ_e and ρ_μ should always be evaluated from experiments simultaneously with their corresponding low-energy parameter η_e and η_μ, respectively, due to the large error correlation between them.[34] The resulting increase in the errors can be more than compensated by including the information of the opening angle in the analysis. Thus errors in the order of a few 10^{-3} could be achieved for ρ_e,ρ_μ and for the hitherto unmeasured η_μ whose value is needed for the derivation of the Fermi coupling constant for the muonic τ decay. The error on the low-energy parameter η_e, however, is hopelessly large; on the other hand, its influence on G_F is negligible.

Most of the errors in Table V compare well with the corresponding errors achieved for μ decay: $\Delta\rho=2.7\times10^{-3}$,[9] $\Delta\eta=13\times10^{-3}$,[8] $\Delta\delta=4.3\times10^{-3}$,[11] and $\Delta\xi=8.4\times10^{-3}$.[27] The errors in Table V have been derived for an ideal detector with 100% solid angle and momentum acceptance, infinitely good angular and

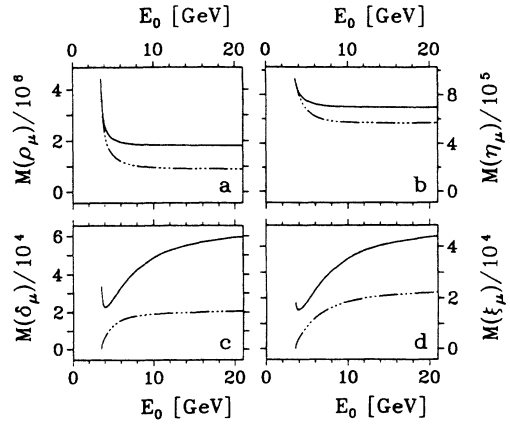

FIG. 15. Total figures of merit for the leptonic decay parameters ρ_μ, η_μ, δ_μ, and ξ_μ as a function of the total beam energy E_0. The curves are derived from the correlated distribution $R(k_\mu,k_e,\cos\theta_{\mu e})$ for the reactions $e^+e^-\to\tau^+\tau^-\to(\mu^+\nu_\mu\bar{\nu}_\tau)(e^-\bar{\nu}_e\nu_\tau)$ by numerical integration.

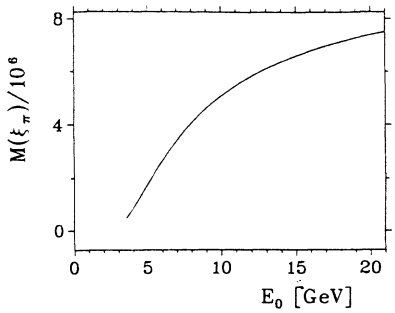

FIG. 17. Total figure of merit for the semileptonic decay parameters ξ_π as a function of the total beam energy E_0. The curve is derived from the correlated distribution $S(k_\pi,k'_\pi)$ for the reactions $e^+e^-\to\tau^+\tau^-\to(\pi^+\bar{\nu}\tau)(\pi^-\nu_\tau)$ by numerical integration.

TABLE V. Statistical errors (in units of 10^{-3}) for the ten different coupling constants and for $P_R^\tau(\mu)$ and $P_R^\tau(e)$, calculated for the distributions $S(k_3,k_4)$ and $R(k_3,k_4,\cos\theta_{34})$ on the basis of an ideal detector and based on 10^7 produced $\tau^+\tau^-$ pairs. They result from a joint analysis of all possible combinations of μ, e, π, and K from decays of $\tau^+\tau^-$ pairs.

Decay parameter	Distribution S		Distribution R	
	4 GeV	10.55 GeV	4 GeV	10.55 GeV
ρ_μ	1.9	2.7	1.7	1.9
η_μ	2.9	3.1	2.9	3.0
δ_μ	36.7	15.3	16.6	11.4
ξ_μ	44.5	15.2	20.3	13.4
$P_R^\tau(\mu)$	17.6	9.6	10.0	6.7
ρ_e	1.9	2.7	1.7	2.0
η_e	508.8	585.9	499.0	529.3
δ_e	36.7	14.4	15.8	11.0
ξ_e	44.8	15.1	20.1	13.3
$P_R^\tau(e)$	17.6	9.1	9.7	6.5
ξ_π	9.3	3.8	8.6	3.8
ξ_K	45.5	19.0	38.0	18.4

momentum resolution and perfect particle identification and background suppression. Thus they constitute a limit for any real detector. The main losses can be expected for the following reasons.

(1) Limits to the emission angle of the charged particles relative to the beam axis because of cylindrical design of the detector or due to deliberate cuts to reduce radiative backgrounds.

(2) Thresholds for particle identification.

(3) Background events, especially due to radiative processes. This will induce severe losses for e^+e^- correlated events and, to some extent, also for $\mu^+\mu^-$ events.

(4) Averaging of the effects due to finite angular and momentum resolution.

In summary an accelerator which produces 10^7 $\tau^+\tau^-$ pairs per year (for example, a τ charm or a B factory) could give results with a precision close to those obtained at the meson factories in the recent decade.

F. Measurement of the μ^+ polarization ξ'_μ

The longitudinal polarization of the μ^+ from τ^+ decay in flight has been derived in Sec. V B. It carries information about the important decay parameter ξ' which cannot be determined by measuring spectral and angular distributions. Here we give a short outline how it could be measured and what precision could be reached.

(1) Positive muons are identified in the main detector.

(2) The decay products of the τ^- signal production and decay of a $\tau^+\tau^-$ pair.

(3) The μ^+ are stopped in a polarimeter outside of the main detector. The polarimeter consists of nondepolarizing material such as aluminum or marble plates, scintillators and an array of drift tubes or proportional chambers to measure the direction of the muons and their decay electrons.

(4) The μ^+ process in a small magnetic field $B \approx 6mT$. The field should be tangential to the (assumed) cylindrical surface of the main detector. Thus two different versions seem feasible: Either a cylindrical field whose axis coincides with the detector axis or a field with field lines parallel to the detector axis.

(5) The e^+ from μ^+ decay obey a forward-backward asymmetry according to the position of its spin at the time of decay. By measuring the time distribution of the decay one can derive the decay asymmetry and thus the muon polarization.

A similar experiment has been performed already at muon momenta of 16 GeV/c for the reaction $\bar{\nu}_\mu \mathrm{Fe} \to X\mu^+$,[35] where the helicity transfer from the $\bar{\nu}_\mu$ onto the μ^+ was measured. There by detecting 3400 events a statistical error on the μ^+ polarization of 20% was reached. In the following this number will be used as a scale factor to estimate the error for the μ^+ polarization from τ^+ decay. In Sec. V formulas (5.2) for the polarization ζ_μ of μ^+ from τ^+ decay and (5.3) for the FM $d\zeta_\mu^2\sigma/dk_\mu$ were derived. Assuming a $V-A$ interaction the corresponding momentum distributions were calculated for a total energy $E_0=4$ GeV and $E_0=10.55$ GeV. They are shown in Figs. 18 and 19. The FM distribution has been normalized to 10^7 events.

In an experiment as sketched above only the region to the right of the maximum can be utilized, because muons of lower energy remain in the central main detector. As an example, we give the rate and error estimation in view of a future B-meson factory:[36]

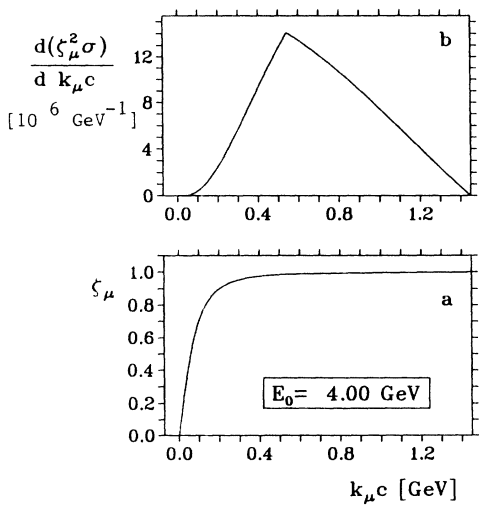

FIG. 18. Polarization ζ_μ and figure of merit $d(\zeta_\mu^2\sigma)/d(k_\mu c)$ for μ^+ from τ^+ decay at 4-GeV total beam energy.

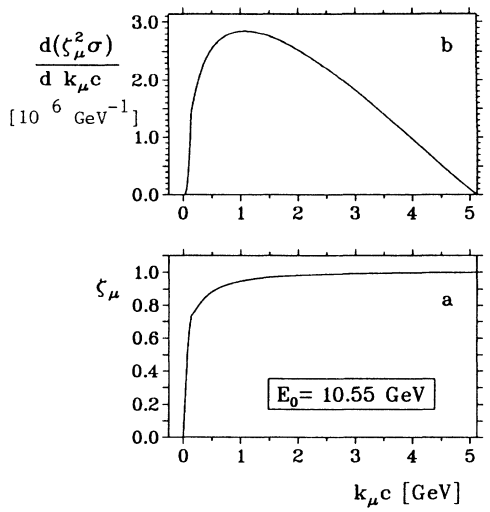

FIG. 19. Polarization ζ_μ and figure of merit $d(\zeta_\mu^2\sigma)/d(k_\mu c)$ for μ^+ from τ^+ decay at 10.55-GeV total beam energy.

(1) residual muon polarization	90%
(2) solid angle	10% of 4π sr
(3) branching ratio τ to μ	18%
(4) τ^- identification	50%
(5) electron detection	25%
(6) muon momentum cut (1 to 2 GeV/c)	25%
(7) useful events per 10^7 $\tau^+\tau^-$ pairs	6000
(8) statistical error on P	$\pm 15\%$

A precision of 15% for the polarization of the μ^+ from τ^+ decay compares well with the precision obtained for the polarization of the e^+ from μ^+ decay. In the era of the synchrocyclotrons the best experiment gave a corresponding error of $\pm 18\%$ for the positron polarization.[37] The meson factories enabled us to reduce their error down to $\pm 4.5\%$ in 1985.[12,38] We emphasize that the measurement of the μ^+ polarization from τ^+ decay is especially rewarding. As a single observable a measurement consistent with $\xi'_\mu = 1$ would give upper limits to five of the ten coupling constants [see Eq. (2.8)], namely, to g^S_{RR}, g^S_{RL}, g^V_{RR}, g^V_{RL}, and to g^V_{RL}, where the coupling constants with mixed coupling RL can only be determined by this measurement. With 15% error the error on, say, g^V_{RR} would be $\Delta g^V_{RR} = \pm 27\%$.

VII. CONCLUSION

It has been shown that the Lorentz structure of the charged weak interaction which manifests itself in the two decays $\tau^+ \to \mu^+ \nu_\mu \bar{\nu}_\tau$ and $\tau^+ \to e^+ \nu_e \bar{\nu}_\tau$ can be determined completely by measuring the τ lifetime (and the corresponding branching ratio), ξ and δ which describe the decay asymmetry, the polarization ξ' of the daughter lepton, and the cross section for inverse τ decay. At an e^+e^- collider with unpolarized beams and c.m. energies between 4 and 15 GeV the first three of these measurements can be performed for both kinds of decay. In addition the polarization ξ'_μ of the μ^+ from τ^+ decay can be measured.

Analytical expressions have been derived for the decay distributions of spin-correlated $\tau^+\tau^-$ pairs in terms of experimentally observable quantities, namely, the momenta of the charged decay products and the opening angle between them. The inclusion of the opening angle greatly enhances the sensitivity, especially for the asymmetry parameters ξ and δ, but also for the spectral shape parameters ρ and η. By numerical integration over the remaining phase space statistical errors for the decay parameters were calculated for an ideal detector. The errors for 10^7 produced $\tau^+\tau^-$ pairs at 10.55 GeV total energy are for the Michel parameters $\Delta\rho_e = \Delta\rho_\mu = 2\times 10^{-3}$, for the low-energy spectrum parameter $\Delta\eta_\mu = 3\times 10^{-3}$, for the differential asymmetry parameters $\Delta\delta_e = \Delta\delta_\mu = 11\times 10^{-3}$, for the integral asymmetry parameters $\Delta\xi_e = \Delta\xi_\mu = 13.4\times 10^{-3}$, and for the probabilities $P^\tau_R(\mu)$ and $P^\tau_R(e)$ of the τ to be right handed $\Delta P^\tau_R(\mu) = 6.7\times 10^{-3}$ and $\Delta P^\tau_R(e) = 6.5\times 10^{-3}$. All of these errors include the effect of the error correlations which are important for the parameter combinations (ρ_e,η_e), (ρ_μ,η_μ), (ξ_e,δ_e), and (ξ_μ,δ_μ). The indices e and μ indicate the particular leptonic decay, and the corresponding decay parameters have *not* been assumed to be equal. (This assumption would reduce the above errors by up to a factor of 2.)

The μ^+ polarization from τ^+ decay can be measured by using the large decay asymmetry of the μ^+ as an analyzer. Here the effective polarization of the μ^+ in the laboratory system was calculated. For a real detector an error of 15% on ξ'_μ is estimated.

We note that up to now only ρ_e and ρ_μ have been measured. While a deviation of their values from the $V-A$ value of $\frac{3}{4}$ would be very exciting, one cannot learn very much if they are equal to $\frac{3}{4}$: Any combination of the six couplings g^S_{LL}, g^S_{LR}, g^S_{RL}, g^S_{RR}, g^V_{RR}, and g^V_{LL} with the remaining four couplings being zero yields this value. In contrast we emphasize again how important it is to measure the pseudoscalar quantities ξ, δ, and ξ', because they *constrain* the coupling constants. For the evaluation of the Fermi coupling constant for the muonic decay of the τ, finally the low-energy parameter η_μ has to be measured.

The errors of most of the parameters quoted above compare quite well with the precision obtained in μ decay experiments. For results close to the $V-A$ predictions they allow us to derive upper limits in the order of 10% for the scalar couplings g^S_{RR} and g^S_{LR}, for the vector couplings g^V_{RR} and g^V_{LR} and for the tensor couplings g^T_{LR} for both leptonic τ decays. The μ^+ polarization measurement with 15% error on ξ^+_μ yields three additional upper limits in the order of 27% for g^S_{RL}, g^V_{RL}, and g^T_{RL}, and also for g^S_{RR} and g^V_{RR}. An η_μ measurement, finally, with an error $\Delta\eta_\mu = 3\times 10^{-3}$ reduces the influence of η on the Fermi coupling constant to the negligible value of 4×10^{-4}. The proposed measurements would thus constitute a considerable improvement of our knowledge about the Lorentz structure of the leptonic charged weak interaction.

ACKNOWLEDGMENTS

The author is especially grateful to Professor H.-J. Gerber for many stimulating discussions and for his encouragement during the entire course of his investigation. It is a pleasure to thank Professor R. Eichler, Dr. T. Nakada, Professor H. Kolanoski, and Professor K. R. Schubert for valuable comments and discussions, Dipl. Phys. K. Göring and M. Dröge for collegial assistance, G. Rudolf for advice on his GRAPHX software.

APPENDIX: EVALUATION OF THE INTEGRALS $M_{\mu\nu}(k_3,k_4,\cos\theta_{34})$ FOR LEPTON-LEPTON CORRELATIONS

The use of the opening angle θ_{34} between the two detected particles as an observable introduces a constraint between the (unobservable) quantities $\cos\theta_3,\cos\theta_4$ and the relative azimuthal angle $\phi_{34}\equiv\phi_4-\phi_3$:

$$\cos\theta_{34}=-\cos\theta_3\cos\theta_4+\sin\theta_3\sin\theta_4\cos\phi_{34}\ . \qquad \text{(A1)}$$

Specifying θ_{34} defines an allowed region in (θ_3,θ_4) space. This region is a rectangle and its interior (see Figs. 20 and 21). Its boundary lines are parallel to the diagonals of the (θ_3,θ_4) diagram. They are obtained for coplanar events ($\cos\phi_{34}=\pm1$), while all of the other events are represented by points in the interior.

This rectangle is important in two ways. First it defines an allowed region in (k_3,k_4) space for a given θ_{34}, and second it confines the region of integration over $\cos\theta_3$ and $\cos\theta_4$ to its interior.

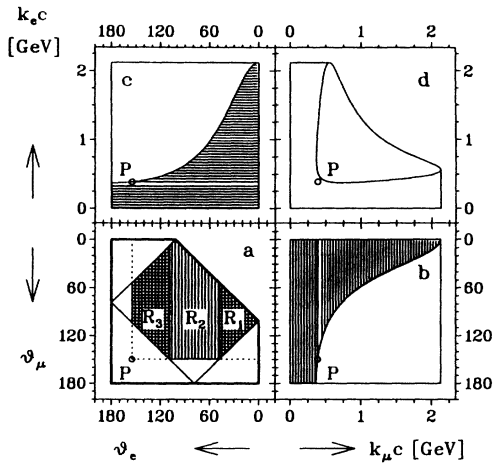

FIG. 21. Kinematics, geometry, and region of integration for the reaction $e^+e^-\to\tau^+\tau^-\to(\mu^+\nu_\mu\bar{\nu}_\tau)(e^-\bar{\nu}_e\nu_\tau)$, $\cos\theta_{\mu e}=-0.6$ and total energy 8 GeV. A point P (momenta k_μ and k_e) is produced for any point of the rectangle in (a) ($0\le\theta_e\le\zeta_e$, $0\le\theta_\mu\le\zeta_\mu$) whose end point (ζ_e,ζ_μ) has also been labeled by P. The selection of a fixed opening angle $\theta_{\mu e}$ between the two momenta constrains the allowed angles θ_μ and θ_π to the oblique rectangle and its interior. The total area in (a) delimited by bold lines is the region for all end points P contributing to the integral. The region of integration is the overlap of the two rectangles. The integrals are different for regions R_1 and R_3 (oblique boundary) on one hand, and for R_2 (horizontal boundary) on the other hand.

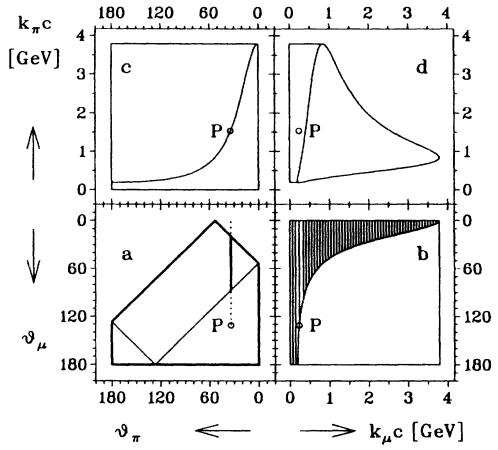

FIG. 20. Kinematics, geometry, and region of integration for the reaction $e^+e^-\to\tau^+\tau^-\to(\mu^+\nu_\mu\bar{\nu}_\tau)(\pi^-\nu_\tau)$, $\cos\theta_{\mu\pi}=-0.6$ and total energy $E_0=8$ GeV. A point P (momenta k_μ and k_π) in (d) is produced for any point of the straight line in (a) ($\theta_\pi=\zeta_\pi, 0\le\theta_\mu\le\zeta_\mu$) whose end point (ζ_π,ζ_μ) has also been labeled by P. The selection of a fixed opening angle $\theta_{\mu\pi}$ between the two momenta constrains the allowed angles θ_μ and θ_π to the oblique rectangle and its interior. The total area in (a) delimited by bold lines is the region for all end points P contributing to the integral. The region of integration is equal to the overlap of line and rectangle and has been marked by a bold line.

The shapes of the region in (k_3,k_4) space depend on the kind of decays: Mesons from two-body decays with a certain momentum k are emitted at a fixed angle ζ, while leptons from three-body decays allow $0\le\theta\le\zeta$ for a given momentum k. Thus for meson-meson correlations a point (k_3,k_4) is transformed to a point (ζ_3,ζ_4) in (θ_3,θ_4) space, for lepton-meson correlations it is transformed to a line in (θ_3,θ_4) space parallel to the lepton angle axis, and for lepton-lepton correlations it is transformed into a rectangle with sides parallel to the axes θ_3 and θ_4.

For lepton-meson correlations one has to integrate over the piece of the line within the rectangle defined by θ_{34}, for lepton-lepton correlations correspondingly over the area common to both rectangles. Figures 20 and 21 show the resulting regions of integration. We do not derive meson-meson correlations for the threefold differential cross section, because this correlation is already fixed by the two-fold differential cross section $d^2\sigma/dk_3dk_4$.

First Integration. We remind the reader that for a point (k_3,k_4) all angles $0\le\cos\theta_3\le\cos\zeta_3$ and $0\le\cos\theta_4\le\cos\zeta_4$ are allowed. The cut of this rectangle in (θ_3,θ_4) space with the rectangle defined by demanding $\cos\theta_{34}$ to be fixed yields up to three different regions R_1, R_2, and R_3 for $\cos\theta_4$ with different boundaries $\Gamma_1(\theta_4)$ and $\Gamma_2(\theta_4)$ for the $\cos\theta_3$ integration. They are given in Table VI,

TABLE VI. Regions R_i and upper and lower boundaries $\Gamma_1(\theta_4)$ and $\Gamma_2(\theta_4)$ for the integration over $\cos\theta_3$.

i	Region R_i for $\cos\theta_4$	$\Gamma_1(\theta_4)$	$\Gamma_2(\theta_4)$
3	$-1\le\cos\theta_4\le-\cos(\theta_{34}-\zeta_3)$	$-\cos(\theta_{34}-\theta_4)$	$-\cos(\theta_{34}+\theta_4)$
2	$-\cos(\theta_{34}-\zeta_3)\le\cos\theta_4\le-\cos(\theta_{34}+\zeta_3)$	$\cos\zeta_3$	$-\cos(\theta_{34}+\theta_4)$
1	$-\cos(\theta_{34}+\zeta_3)\le\cos\theta_4\le+1$	$-\cos(\theta_{34}-\theta_4)$	$-\cos(\theta_{34}+\theta_4)$

and Fig. 21 shows an example where all three regions contribute.

For region R_1 and R_3 we obtain the definite integrals

$$K_0(\theta_4)=\pi\ ,$$
$$K_1(\theta_4)=-\pi\cos\theta_4\cos\theta_{34}\ , \tag{A2}$$
$$K_2(\theta_4)=\frac{\pi}{2}[(3\cos^2\theta_{34}-1)\cos^2\theta_4+\sin^2\theta_{34}]\ .$$

For region R_2, the definite integrals are

$$K_0(\theta_4)=\frac{\pi}{2}-X(\theta_4)\ ,$$
$$K_1(\theta_4)=W(\theta_4)-\cos\theta_4\cos\theta_{34}\left[\frac{\pi}{2}-X(\theta_4)\right]\ , \tag{A3}$$
$$K_2(\theta_4)=\tfrac{1}{2}(\cos\zeta_3-3\cos\theta_4\cos\theta_{34})W(\theta_4)+\tfrac{1}{2}[(3\cos^2\theta_{34}-1)\cos^2\theta_4+\sin^2\theta_{34}]\left[\frac{\pi}{2}-X(\theta_4)\right]$$

with

$$X(\theta_4)=\arcsin\frac{\cos\zeta_3+\cos\theta_4\cos\theta_{34}}{\sin\theta_4\sin\theta_{34}} \tag{A4}$$

TABLE VII. Contribution of the different regions to the integral.

$\cos\theta_{34}$	$\cos\zeta_3$	$\cos\zeta_4\in$ R_1	R_2	R_3
<0	$=-1$	I_3+I_1		i_1
	$<+\cos\theta_{34}$	$i_3+I_2^{(3)}+I_1$	$i_2^{(3)}+I_1$	i_1
	$=+\cos\theta_{34}$		$i_2^{(1)}+I_1$	i_1
	$<-\cos\theta_{34}$		$i_2^{(3)}+I_1$	i_1
	$=-\cos\theta_{34}$		$i_2^{(2)}$	
	$<+1$		$i_2^{(3)}$	
$=0$	$=-1$	I_3+I_1		i_1
	<0	$i_3+I_2^{(3)}+I_1$	$i_2^{(3)}+I_1$	i_1
	$=0$		$i_2^{(4)}$	
	$<+1$		$i_2^{(3)}$	
>0	$=-1$	I_3+I_1		i_1
	$<-\cos\theta_{34}$	$i_3+I_2^{(3)}+I_1$	$i_2^{(3)}+I_1$	i_1
	$=-\cos\theta_{34}$	$i_3+I_2^{(2)}$	$i_2^{(2)}$	
	$<+\cos\theta_{34}$	$i_3+I_2^{(3)}$	$i_2^{(3)}$	
	$=+\cos\theta_{34}$		$i_2^{(1)}$	
	<1		$i_2^{(3)}$	

and

$$W(\theta_4)=\sqrt{\sin^2\zeta_3\sin^2\theta_4-(\cos\theta_{34}+\cos\zeta_3\cos\theta_4)^2}\ . \tag{A5}$$

Second Integration. Generally, each of the integrals $M_{\mu\nu}$ is composed of at most three parts evaluated in regions R_1, R_2, and R_3 as shown in Table VII. A specific value of ζ_3 corresponds to a horizontal line in the (θ_3,θ_4) diagram which cuts the rectangle defined by $\cos\theta_{34}$. Integrals extending over the full region have been labeled I_1, $I_2^{(n)}$ $(n=1,\ldots,4)$, and I_3, where n depends on $\cos\theta_{34}$ and $\cos\zeta_3$ (see below). Integrals extending over only part of a region (due to the cut $\cos\theta_4\ge\cos\zeta_4$) are labeled correspondingly by i_1, $i_2^{(n)}$, and i_3. The limits of integration for the three regions are given in Table VIII.

For abbreviation we have used $\cos\Theta_l=-\cos(\theta_{34}-\zeta_3)$ and $\cos\Theta_h=-\cos(\theta_{34}+\zeta_3)$. The indefinite integrals in regions R_1 and R_3, to be taken in the limits of Table VIII, are

$$M_{0\nu}=\pi f_1^{(\nu)}(\theta_4)\ ,$$
$$M_{1\nu}=\pi\cos\theta_{34}f_1^{(\nu+1)}(\theta_4)\ , \tag{A6}$$
$$M_{2\nu}=\frac{\pi}{2}[(3\cos^2\theta_{34}-1)f_1^{(\nu+2)}(\theta_4)+\sin^2\theta_{34}f_1^{(\nu)}(\theta_4)]\ ,$$

where

$$f_1^{(\nu)}(\theta_4)=\frac{\cos^{\nu+1}(\theta_4)}{\nu+1}\ .$$

The integrals in region R_2 are somewhat more complicated. Their type furthermore depends on the values of $\cos\theta_{34}$ and $\cos\zeta_4$. Table IX lists the conditions for the different types of integrals and the values of the coefficients α_1, α_2, c_1, and c_2 which parametrize the integrals $I_2^{(1)}$ to $I_2^{(4)}$ (see below).

The indefinite integrals $I_2^{(1)}$ to $I_2^{(4)}$, to be taken in the limits of Table VIII, are

TABLE VIII. Upper and lower boundaries for the $\cos\theta_4$ integration in the three different regions.

Region	Limits for $\cos\theta_4$ Full region (I_ν)	Partial region (i_ν)
R_3	$[-1,\cos\Theta_l]$	$[\cos\zeta_4,\cos\Theta_l]$
R_2	$[\cos\Theta_l,\cos\Theta_h]$	$[\cos\zeta_4,\cos\Theta_h]$
R_1	$[\cos\Theta_h,+1]$	$[\cos\zeta_4,+1]$

TABLE IX. Types of integrals for region R_2 in functions of ζ_3.

Integral	Condition for ζ_3	c_1	α_1	c_2	α_2
$I_2^{(1)}$	$\zeta_3=\theta_{34}\neq 90°$	1	$-\dfrac{1}{\cos\theta_{34}}$	0	
$I_2^{(2)}$	$\zeta_3+\theta_{34}=180°$	0		1	$\dfrac{\cos\theta_{34}}{\sin\theta_{34}-\sin\zeta_3}$
$I_2^{(3)}$	$\zeta_3\neq\theta_{34}$	1	$-\dfrac{\sin\theta_{34}+\sin\zeta_3}{\sin(\theta_{34}+\zeta_3)}$	1	
$I_2^{(4)}$	$\zeta_3=\theta_{34}=90°$	0		0	

$$M_{0\nu}=\frac{\pi}{2}f_1^{(\nu)}-f_2^{(\nu)}-f_3^{(\nu)}\ ,$$

$$M_{1\nu}=\cos\theta_{34}\left[-\frac{\pi}{2}f_1^{(\nu+1)}+f_2^{(\nu+1)}+f_3^{(\nu+1)}\right]+(f_4^{(\nu)}+f_5^{(\nu)})\ , \tag{A7}$$

$$M_{2\nu}=\frac{1}{2}\left[(3\cos^2\theta_{34}-1)\left[\frac{\pi}{2}f_1^{(\nu+2)}-f_2^{(\nu+2)}-f_3^{(\nu+2)}\right]+\sin^2\theta_{34}\left[\frac{\pi}{2}f_1^{(\nu)}-f_2^{(\nu)}-f_3^{(\nu)}\right]\right]$$
$$+\tfrac{1}{2}[\cos\zeta_3(f_4^{(\nu)}+f_5^{(\nu)})-3\cos\theta_{34}(f_4^{(\nu+1)}+f_5^{(\nu+1)})]$$

with

$$f_1^{(\nu)}=\frac{\cos^{(\nu+1)}\theta_4}{\nu+1}\ , \tag{A8}$$

$$f_2^{(\nu)}=+X(\theta_4)\frac{\cos^{(\nu+1)}\theta_4}{\nu+1}\ , \tag{A9}$$

$$f_3^{(\nu)}=-\frac{c_1Y_1^{(\nu)}+c_2Y_2^{(\nu)}}{\nu+1}\ , \tag{A10}$$

$$f_4^{(\nu)}=W(\theta_4)\frac{\cos^{(\nu+1)}\theta_4}{\nu+1}\ , \tag{A11}$$

$$f_5^{(\nu)}=\frac{R^{(\nu)}}{\nu+1}\ . \tag{A12}$$

The functions $R^{(\nu)}$ and $Y_i^{(\nu)}$ are derived from partial integration of $W(\theta_4)\cos^\nu(\theta_4)$ and $X(\theta_4)\cos^\nu\theta_4$, respectively:

$$R^{(\nu)}=\sum_{\rho=0}^{\nu+1}\begin{bmatrix}\nu+1\\ \rho\end{bmatrix}\cos^{\nu+1-\rho}\Theta_h(\cos\Theta_l-\cos\Theta_h)^{\rho+1}(2\mathcal{L}_{\rho+2}-\mathcal{L}_{\rho+1})\ ,$$

$$Y_1^{(\nu)}=-\arctan\frac{s}{\alpha_1}+\alpha_1(1-\cos\Theta_h)\sum_{\lambda=0}^{\nu}\sum_{\rho=\lambda}^{\nu}\begin{bmatrix}\rho\\ \lambda\end{bmatrix}\cos^{\rho-\lambda}\Theta_h(\cos\Theta_l-\cos\Theta_h)^\lambda\mathcal{L}_{\lambda+1}\ ,$$

$$Y_2^{(\nu)}=(-1)^\nu\left[-\arctan\frac{s}{\alpha_2}+\alpha_2(1+\cos\Theta_h)\sum_{\lambda=0}^{\nu}\sum_{\rho=\lambda}^{\nu}\begin{bmatrix}\rho\\ \lambda\end{bmatrix}(-1)^\rho\cos^{\rho-\lambda}\Theta_h(\cos\Theta_l-\cos\Theta_h)^\lambda\mathcal{L}_{\lambda+1}\right]\ ,$$

$$\mathcal{L}_1=\arctan s,\quad \mathcal{L}_{\nu+1}=\int\frac{ds}{(s^2+1)^{\nu+1}},\quad \mathcal{L}_{\nu+1}=\frac{s}{2\nu(s^2+1)^\nu}+\frac{2\nu-1}{2\nu}\mathcal{L}_\nu$$

and

$$s=\left[\frac{\cos\theta_4-\cos\Theta_l}{\cos\Theta_h-\cos\theta_4}\right]^{1/2}.$$

The indefinite integrals $I_2^{(4)}$ (for $\zeta_3=\theta_{34}=90°$) finally are given by

$$M_{0\nu}=\frac{\pi}{2}f_1^{(\nu)}(\theta_4)\ ,$$
$$M_{10}=\tfrac{1}{2}(-\theta_4+\sin\theta_4\cos\theta_4)\ ,$$
$$M_{11}=-\tfrac{1}{3}\sin^3\theta_4\ , \tag{A13}$$
$$M_{12}=\tfrac{1}{8}[-\theta_4+\sin\theta_4\cos\theta_4(\cos^2\theta_4-\sin^2\theta_4)]\ ,$$
$$M_{2\nu}=\frac{\pi}{4}[f_1^{(\nu)}(\theta_4)-f_1^{(\nu+2)}(\theta_4)]\ .$$

[1]W. Fetscher, H.-J. Gerber, and K. F. Johnson, Phys. Lett. B **173**, 102 (1986).

[2]F. Scheck, Phys. Rep. **44**, 204 (1978).

[3]S. Weinberg, Phys. Rev. Lett. **19**, 1264 (1967); A. Salam, in *Elementary Particle Theory: Relativistic Groups and Analyticity (Nobel Symposium No. 8)*, edited by N. Svartholm (Almqvist and Wiksell, Stockholm, 1969), p. 367; and S. L. Glashow, J. Iliopoulos, and L. Maiani, Phys. Rev. D **2**, 1285 (1970).

[4]L. Michel, Proc. Phys. Soc. London **A63**, 514 (1950).

[5]F. Scheck, *Lepton, Hadrons and Nuclei* (North-Holland, Amsterdam, 1983).

[6]K. Mursula and F. Scheck, Nucl. Phys. **B254**, 189 (1985).

[7]T. Kinoshita and A. Sirlin, Phys. Rev. **108**, 844 (1957).

[8]H. Burkard, F. Corriveau, J. Egger, W. Fetscher, H.-J. Gerber, K. F. Johnson, H. Kaspar, H. J. Mahler, M. Salzmann, and F. Scheck, Phys. Lett. **160B**, 343 (1985).

[9]S. E. Derenzo, Phys. Rev. **181**, 1854 (1969).

[10]J. Carr, G. Gidal, B. Gobbi, A. Jodidio, C. J. Oram, K. A. Shinsky, H. M. Steiner, D. P. Stoker, M. Strovink, and R. D. Tripp, Phys. Rev. Lett. **51**, 627 (1983); H. M. Steiner (private communication).

[11]B. Balke *et al.*, in *Proceedings of the 22nd International Conference on High Energy Physics*, Leipzig, East Germany, 1984, edited by A. Meyer and E. Wieczorek (Akademie der Wissenschaften der DDR, Zeuthen, 1984), Vol. 1, p. 208.

[12]H. Burkard, F. Corriveau, J. Egger, W. Fetscher, H.-J. Gerber, K. F. Johnson, H. Kaspar, H. J. Mahler, M. Salzmann, and F. Scheck, Phys. Lett. **150B**, 242 (1985).

[13]C. Jarlskog, Nucl. Phys. **75**, 659 (1966).

[14]CHARM Collaboration, F. Bergsma *et al.*, Phys. Lett. **122B**, 465 (1983).

[15]K. Mursula, M. Roos, and F. Scheck, Nucl. Phys. **B219**, 321 (1983).

[16]W. Fetscher, Phys. Lett. **140B**, 117 (1984).

[17]L. Ph. Roesch *et al.*, Helv. Phys. Acta **55**, 74 (1982).

[18]A. I. Alikhanov *et al.*, Zh. Eksp. Teor. Fiz. **38**, 1918 (1960) [Sov. Phys. JETP **11**, 1380 (1960)]; G. Backenstoss *et al.*, Phys. Rev. Lett. **6**, 415 (1961); M. Bardon *et al.*, *ibid.* **7**, 23 (1961); A. Possoz *et al.*, *ibid.* **B70**, 265 (1977); R. Abela *et al.*, Nucl. Phys. **A39**, 413 (1983).

[19]W. Fetscher, in *Neutrino 86: Neutrino Physics and Astrophysics*, proceedings of the 12th International Conference, Sendai, Japan, 1986, edited by T. Kitagaki and H. Yuta (World Scientific, Singapore, 1986).

[20]T. D. Lee and C. N. Yang, Phys. Rev. **108**, 1611 (1957).

[21]J. Missimer, F. Scheck, and R. Tegen, Nucl. Phys. **B188**, 29 (1981).

[22]ARGUS Collaboration, H. Albrecht *et al.*, Phys. Lett. B **202**, 149 (1988).

[23]S. M. Berman, Phys. Rev. **112**, 267 (1958); T. Kinoshita and A. Sirlin, *ibid.* **113**, 1652 (1959); S. M. Berman and A. Sirlin, Ann. Phys. (N.Y.) **20**, 20 (1962); Ref. 2.

[24]W. Fetscher, in Proposal for a *B*-Meson Factory, PSI Report No. PR-88-09, 1988 (unpublished).

[25]For a recent review, see, for example, B. C. Barish and R. Stroynowski, Phys. Rep. **157**, 1 (1988); K. K. Gan and M. L. Perl, Int. J. Mod. Phys. A **3**, 531 (1988).

[26]H.-J. Gerber, in *Proceedings of the International Europhysics Conference on High Energy Physics*, Uppsala, Sweden, 1987, edited by O. Bottner (European Physical Society, Petit-Lancy, Switzerland, 1987).

[27]I. Beltrami, H. Burkard, R. D. von Dincklage, W. Fetscher, H.-J. Gerber, K. F. Johnson, E. Pedroni, M. Salzmann, and F. Scheck, Phys. Lett. B **194**, 326 (1987).

[28]Y. S. Tsai, Phys. Rev. D **4**, 2821 (1971).

[29]H. Kühn and F. Wagner, Nucl. Phys. **B236**, 16 (1984).

[30]M. L. Perl *et al.*, Phys. Lett. **35**, 1489 (1975).

[31]So-Young Pi and A. I. Sanda, Ann. Phys. (N.Y.) **106**, 171 (1977).

[32]A more specialized treatment of leptonic decay parameters for the $Z^0 \to \pi^+ \tau^-$ decay is given in C. A. Nelson, Phys. Rev. D **40**, 123 (1989).

[33]Particle Data Group, G. P. Yost *et al.*, Phys. Lett. B **204**, 1 (1988).

[34]For single-lepton spectra from unpolarized muons, the correlation coefficient between ρ_μ and η_μ (ρ_e and η_e) is found to be $+55\%$ for a total energy $E_0 = 4$ GeV and $+35\%$ for $E_0 = 10.55$ GeV.

[35]M. Jonker *et al.*, Phys. Lett. **86B**, 229 (1979).

[36]Proposal for a *B*-Meson Factory, PSI Report No. PR-88-09, 1988 (unpublished).

[37]J. Duclos, H. Heintze, A. de Rújula, and V. Soergel, Phys. Lett. **9**, 62 (1964).

[38]F. Corriveau, J. Egger, W. Fetscher, H.-J. Gerber, K. F. Johnson, H.-J. Mahler, M. Salzmann, H. Kaspar, and F. Scheck, Phys. Rev. D **24**, 2004 (1981).